Journal of Neuroscience Methods 384 (2023) 109745

Contents lists available at ScienceDirect

Journal of Neuroscience Methods

journal homepage: www.elsevier.com/locate/jneumeth

A review on Alzheimer's disease classification from normal controls and mild cognitive impairment using structural MR images

Neha Garg [a,*], Mahipal Singh Choudhry [a], Rajesh M Bodade [b]

[a] Delhi Technological University, Department of Electronics and Communication, Delhi 110042, India
[b] Military College of Telecommunication Engineering (MCTE), Mhow, Indore 453441, Madhya Pradesh, India

ARTICLE INFO

Keywords:
Alzheimer's disease
ROI-based method
Voxel-based morphometry
Vertex-based methods
Wavelet Transform-based method
Classification

ABSTRACT

Alzheimer's disease (AD) is an irreversible neurodegenerative brain disorder that degrades the memory and cognitive ability in elderly people. The main reason for memory loss and reduction in cognitive ability is the structural changes in the brain that occur due to neuronal loss. These structural changes are most conspicuous in the hippocampus, cortex, and grey matter and can be assessed by using neuroimaging techniques viz. Positron Emission Tomography (PET), structural Magnetic Resonance Imaging (MRI) and functional MRI (fMRI), etc. Out of these neuroimaging techniques, structural MRI has evolved as the best technique as it indicates the best soft tissue contrast and high spatial resolution which is important for AD detection. Currently, the focus of researchers is on predicting the conversion of Mild Cognitive Impairment (MCI) into AD. MCI represents the transition state between expected cognitive changes with normal aging and Alzheimer's disease. Not every MCI patient progresses into Alzheimer's disease. MCI can develop into stable MCI (sMCI, patients are called non-converters) or into progressive MCI (pMCI, patients are diagnosed as MCI converters). This paper discusses the prognosis of MCI to AD conversion and presents a review of structural MRI-based studies for AD detection. AD detection framework includes feature extraction, feature selection, and classification process. This paper reviews the studies for AD detection based on different feature extraction methods and machine learning algorithms for classification. The performance of various feature extraction methods has been compared and it has been observed that the wavelet transform-based feature extraction method would give promising results for AD classification. The present study indicates that researchers are successful in classifying AD from Normal Controls ($N_{rm}C$) but, it still requires a lot of work to be done for MCI/ $N_{rm}C$ and MCI/AD, which would help in detecting AD at its early stage.

1. Introduction

Alzheimer's disease (AD) is a chronic neurodegenerative brain disorder that is characterized by the continuous loss of memory and cognitive ability. This irreversible progressive brain disorder has now become the pedigree of 60% to 70% of cases of dementia which progresses slowly in beginning and is exacerbated over time (Brookmeyer et al., 2007). AD occurs due to the accumulation of amyloid beta [Aβ] peptides in the form of amyloid plaques and tau proteins as neurofibrillary tangles in the brain (Zhang et al., 2011). The process slowly leads to the non-functionality of healthy neurons and breaks the neural circuit (Yang et al., 2019). The initial neuronal loss occurs in the region of the hippocampus, amygdala, and entorhinal cortex (Moon et al., 2018; Juottonen et al., 1998; Barnes et al., 2006). These regions control the formation of memory. Gradually, neuronal loss spreads to other regions of the brain and causes volumetric reduction (Sur et al., 2020).

In AD patients, the pathophysiological changes in the brain set up the roots for cognitive, functional, and behavioral challenges much before the beginning of clinical symptoms (Jack et al., 2010; McCarthy et al., 2019). Major clinical symptoms of AD are amnesia, lack of communication, absent-mindedness, futility, and personality disorder. There are some treatments that can delay the progression of AD but presently there is no effective treatment that can completely cure this disease. Therefore, precise detection of AD is required at the earliest i.e., at Mild Cognitive Impairment (MCI) stage (Sperling et al., 2011; Davatzikos et al., 2008a). Presently, MCI is also not completely curable due to inaccurate diagnosis which mainly depends on psychological tests such as Clock Test, Mini-Mental State Examination (MMSE), Functional

* Corresponding author.
E-mail addresses: ngcoolneha@gmail.com (N. Garg), msc_1976@yahoo.com (M.S. Choudhry), rajeshbodade@gmail.com (R.M. Bodade).

https://doi.org/10.1016/j.jneumeth.2022.109745
Received 4 February 2022; Received in revised form 4 October 2022; Accepted 11 November 2022
Available online 14 November 2022

Activities Questionnaire (FAQ), and Clinical Dementia Rating (CDR) (Morris, 1993; Kukull et al., 1994). All these tests consume a lot of time and are not much accurate. Since every MCI patient does not progress into Alzheimer therefore, it is essential to develop advanced automated techniques that can interpret whether MCI patients will develop AD or not (Misra et al., 2009). MCI patients progressing into AD are called progressive Mild Cognitive Impairment (pMCI) patients while those who remain stable or revert to normal cognition are called stable Mild Cognitive Impairment (sMCI) patients. Low classification accuracy is observed between sMCI and pMCI due to the heterogeneity of cortical thinning patterns in sMCI patients (Tang et al., 2014; Cuingnet et al., 2011). So, the need of the hour is to increase the classification accuracy for sMCI/pMCI.

This paper includes the survey on feature extraction techniques based on voxel-based analysis, vertex-based analysis, ROI-based analysis, wavelet transform-based analysis, texture-based analysis, and machine learning techniques viz. Support Vector Machine (SVM), Naive Bayes, Artificial Neural Network (ANN), Nearest Neighbor, and Random Forest. This study focuses on Structural MR images as these are better than the other existing neuro-imaging modalities. This technique provides the internal structural details of the brain so this can easily capture the AD atrophies like reduction in hippocampus volume, and size, decrease in cortical thickness, and enlargement of ventricles (Teipel et al., 2013). Researchers are also focusing on other modalities such as fMRI (Odusami et al., 2021) and Diffusion Tensor Imaging (Lella et al., 2021) which are good for detecting metabolic activities and white matter density respectively.

This paper is organized as follows: Section 2 describes the biomarkers for AD. In Section 3 we present different feature extraction techniques. Section 4 discusses different classifiers used for AD detection. Section 5 presents recent trends in AD detection. Various challenges in AD detection are discussed in Section 6 while Section 7 concludes this review along with future directions.

2. Biomarkers for Alzheimer's disease

A biomarker is a biological neurochemical, measurable indicator that is used to detect the presence of disease (Hampel et al., 2010; Gerardin et al., 2009). Several new biomarkers are being examined to diagnose AD at its initial stage i.e., at its MCI stage. The broad category of biomarkers includes neuroimaging features and cerebrospinal fluid (CSF). These biomarkers are the indicators of structural atrophies of the AD brain which are responsible for cognitive impairment (Buchanan et al., 1998). These biomarkers can also be partitioned according to their relevance for the distinctive physio-pathological groups such as cerebral amyloid deposition, tau pathology, and neurodegeneration (Jagust et al., 2009).

2.1. Biomarker-neuroimaging

Neuroimaging techniques are used to show the inner structural details of the human body and thus very conveniently give information about the size, volume, and shape of the brain tissue. These techniques help in assessing the growth and extremity of disease in the brain of patients suffering from AD (Frisoni et al., 2010). In this disease, initially, the neurons in the entorhinal cortex and hippocampus part of the brain get damaged which leads to reduction in the hippocampus (Chupin et al., 2009) and cortical surface volume (Sabuncu et al., 2011). It later affects other regions of the brain which in turn reduces the size of the brain. Due to this reduced size, cerebral ventricles start appearing larger than their normal size (Nestor et al., 2008). These changes are considered biomarkers for the early detection of neurodegenerative disorders (Khoury and Ghossoub, 2019; Blennow, 2004). Structural MRI (sMRI) is a very popular and effective technique used to predict the clinical assessment of AD and MCI patients (Killiany et al., 2000; Vemuri et al., 2010). Magnetic Resonance Imaging does not use ionizing radiation and provides information for different types of tissues (Glodzik-Sobanska et al., 2005). It is to be noted that both T1 -weighted MR images and T2 -weighted MR images are used by researchers in their work (Kamathe et al., 2018). A sample of MR images for Normal Person, MCI, and AD has been extracted from (Chandra et al., 2019) and is illustrated in Fig.1.

2.2. Biomarker- cerebrospinal fluid

Cerebrospinal Fluid (CSF) is a liquid that fills the extracellular compartment of the brain, spinal cord, subarachnoid space, cerebral ventricles, cerebral cisterns, and lumbar cistern. In the initial phase of AD, synaptic loss occurs with the deposition of amyloid-beta [Aβ] and tau proteins (Davatzikos et al., 2011) that highly influence the CSF level in brain tissue. Blennow (2004) reviewed the performance of three biomarkers viz. total tau(T-tau), the 42 amino acid form of amyloid-beta [Aβ], and phosphorylated tau (P-tau) for AD diagnosis. The authors concluded that CSF protein biomarkers might have clinical utility for AD diagnosis. In addition, a combination of biomarkers gives better accuracy for AD diagnosis in comparison to a single biomarker.

3. Feature extraction methods

Feature extraction is a technique used to extract informative features from images. The feature is a basic entity that represents the image. Efficient feature extraction provides fast training of the model, reduces the processing time, and hence gives better classification accuracy. The classification accuracy of machine learning algorithms with structural imaging studies like MRI also depends largely on feature extraction. AD Detection includes extracting features, selecting informative features to remove redundancy, reducing the feature dimensions, and then using classifiers for classification. Effective features for AD detection are hippocampal shape, hippocampal area, and hippocampal volume, grey matter density maps, cortical thickness, cortical curvature, cortical surface area, and texture features such as histogram, entropy, and energy. These features can be extracted through different feature extraction methods. Fig. 2 shows an AD detection system with different feature extraction methods that is used to diagnose AD at the initial stage. The following techniques are preferably used for extracting features for AD classification:

- Pre-defined Region of Interest (ROIs)- based approaches
- Voxel-Based Morphometry (VBM), or Voxel-based segmented tissue density maps
- Cortical surface or Vertex-based method
- Wavelet Transform-based method
- Texture-based method

3.1. Pre-defined ROI- based approaches

Application of a ROI technique requires a priori data and expert knowledge about the magnitude and spatial pattern of disease. This technique helps in extracting features from part of the brain which is highly affected by the disease. The structural atrophies are visualized through cortical thinning, hippocampal volume reduction, and ventricle enlargement. Manual segmentation of ROIs is done by experts in several thin brain slices and is thus a time-consuming activity. The efficiency of the manual method relies on the prior knowledge of AD acquired by the experts based on the studies previously conducted on imaging data (Elsayed et al., 2012). Automatic methods involve the use of Atlas for labeling the MR images. These methods have not been effective, as there were variabilities found from patient to patient. Hence, investigators are required to segment the image manually (Rana et al., 2015). Hippocampal features are key aspects of ROI based techniques. These features are described in the following section.

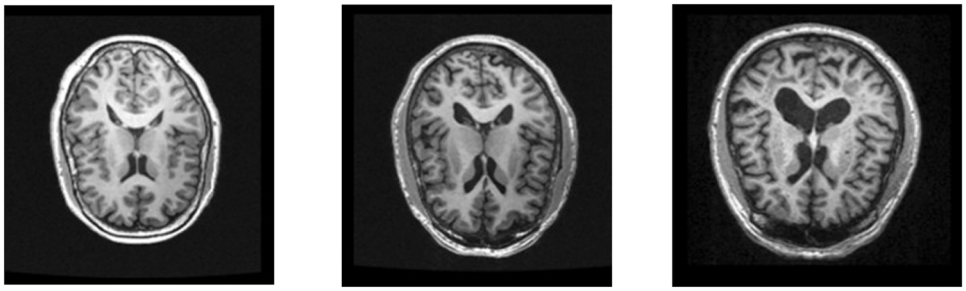

(a) (b) (c)

Fig. 1. Sample MR image (a) Normal Person (b) MCI (c) AD (Chandra et al., 2019).

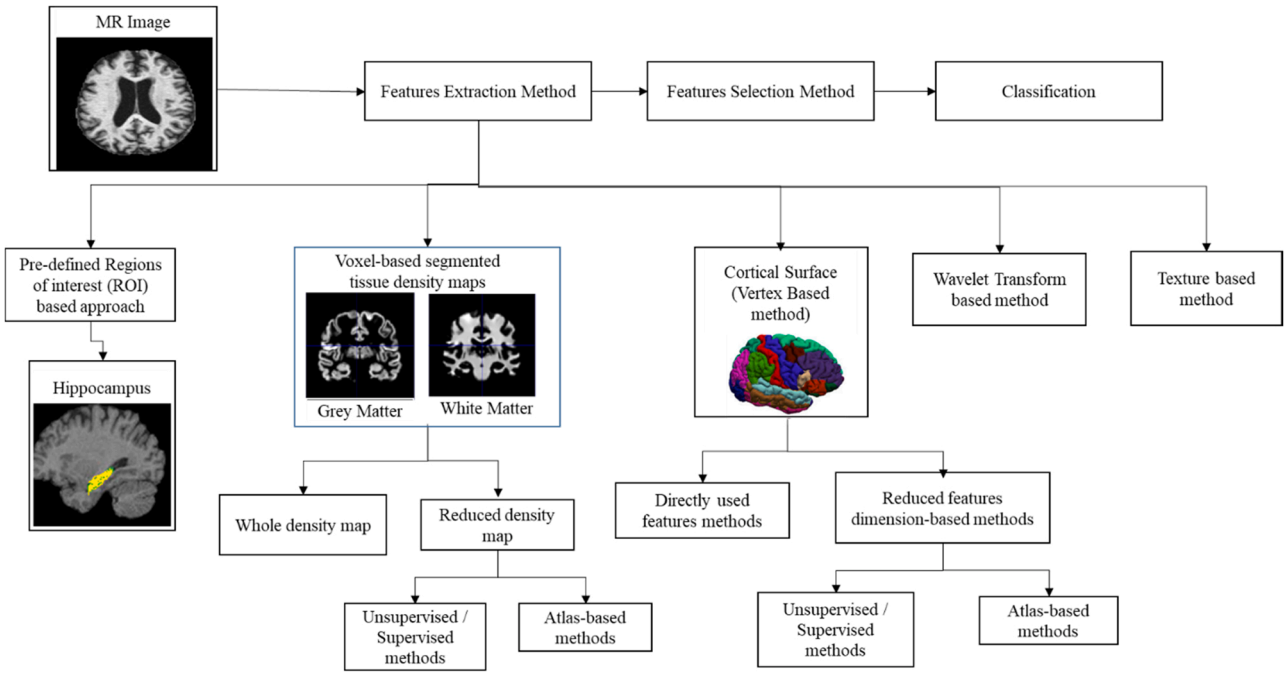

Fig.2. AD detection system with feature extraction methods.

3.1.1. *Hippocampal features*

The hippocampus is located deep in the temporal lobe and is majorly influenced by AD (Jaroudi et al., 2017). Structural atrophies of the hippocampus have emerged as valuable trademarks in feature extraction for AD, MCI, and $N_{rm}C$ classification (Killiany et al., 2002) (Hampel et al., 2010) (Chupin et al., 2009). Reduction in hippocampal volume is widely used as a biomarker for AD detection (Jack et al., 2011). Besides this, the amygdala (Poulin et al., 2011), the ventricles, and the whole brain (Tanabe et al., 1997) are other regions of importance.

Uysal and Ozturk (2020) used hippocampal volume reduction as a biomarker. The authors used ITK-SNAP software (Almuzian et al., 15 Feb. 2018; Yushkevich et al., 2016) to carry out the analysis and obtained significant results with the model having the combination of biomarkers viz. left and right hippocampal volume, age, and gender. Sørensen et al. (2016) combined different biomarkers related to hippocampal shape, hippocampal texture, cortical thickness measurement, and volumetric measurement for multiclass classification of AD, $N_{rm}C$, and MCI. The authors used Freesurfer volumetry (Fischl et al., 2002) for volumetric and cortical thickness measurements. The leftward and dextral hippocampus were extracted individually by applying a non-local patch multi-atlas-based segmentation technique (Coupé et al., 2011). Leftward and dextral hippocampal shape labels were computed by marking 30 surface landmarks across the surface of the segmented hippocampus (Achterberg et al., 2014). The hippocampal texture features were the histograms computed through Gaussian filter response from both hippocampus (Sørensen et al., 2012). This study showed that hippocampal texture features emerge as the best candidate feature accompanied by a volume of the hippocampus, volume of ventricles, and parietal lobe thickness. Baskar et al. (2019) worked on texture and shape features obtained from the posterior cingulate cortex and hippocampus. Out of total 457 features, 447 were texture features and 10 were shape features. Further, a multiple-criterion feature selection method was used by the authors for selecting 19 appropriate features for AD classification. The authors combined two classifiers viz. Back-Propagation Artificial Neural Network (BPANN) and Kernel Fuzzy C-Means Clustering (KFCM) to enhance classification accuracy. Wang et al. (2006) observed the pattern of hippocampal surface variation for healthy subjects and mild AD patients. The authors divided the hippocampal surface into three zones viz. a superior zone including CA2, CA3, CA4 subfields and the gyrus dentatus, a lateral zone including CA1 subfield, and an inferior medial zone including the subiculum using a hippocampal template. They concluded that variations in CA1 subfield and subiculum are more promising biomarkers than variations in CA2, CA3, CA4 subfields and gyrus dentus in mild AD/ $N_{rm}C$ classification. Colliot et al. (2008) used

normalized hippocampus volumes as a biomarker for AD classification. The authors calculated the average normalized hippocampal volumes of both hemispheres for AD/ $N_{rm}C$ and AD/MCI classification. Gerardin et al. (2009) used spherical harmonic coefficients to find hippocampal shapes and SVM to classify AD from $N_{rm}C$ and MCI. Farhan et al. (2014) used hippocampus size as a feature for AD classification with an ensemble mode of classifiers. The authors compared the performance of different features viz. grey matter volume, white matter volume, CSF volume, volume of grey matter +white matter + CSF, area of left hippocampus, area of right hippocampus, area of right and left hippocampus, and combination of features. They concluded that area of the left hippocampus when used as a feature produced the best result. Wang et al. (2007) used large-deformation diffeomorphic metric mapping and principal component analysis for AD/MCI classification and obtained 81.1% accuracy. Since manual segmentation of the hippocampus is very difficult due to the complex structure of the brain, Chupin et al. (2009) in 2009 proposed a completely automatic method based on probabilistic and structural preliminaries required for segmenting the hippocampus. The authors used hippocampal volume as a feature to classify AD and MCI. Ben Ahmed et al. (2015) proposed an approach that deals with the fusion of two biomarkers: visual features of the hippocampus and CSF. The authors obtained an accuracy of 87.0% in AD/ $N_{rm}C$ classification on the ADNI dataset. Table 1 lists the prominent studies for AD classification with $N_{rm}C$ and MCI using ROI-based approaches.

Table 1 indicates that hippocampal texture and volumetric features produce more promising AD classification results than features related to hippocampal shape and size (Luk et al., 2018). Shape features suffer from high dimensionality and are noisy, hence, not reliable (Park et al., 2012). These features produce significantly better results when their dimensions are reduced (Park et al., 2012). It has been observed that ROI based method faces difficulty in capturing the hippocampal features accurately from the complex structure of the brain (Khan et al., 2008;

Table 1
Performance comparison of prominent studies for AD classification with $N_{rm}C$ and MCI using ROI-based approaches.

Author	Data Set	DataBase	Feature Type	Classifier	Performance	Observations
Baskar et al. (2019)	AD=137 $N_{rm}C$=162 MCI=210	ADNI	Texture and shape features from the hippocampus and Posterior Cingulate Cortex	BPANN + KFCM	**AD / $N_{rm}C$** (ACY=98.7, SNY=79.6, SPY=85.6)	Shape features suffer from the problem of high dimensionality, are noisy, and hence not reliable (Park et al., 2012)
					MCI/ $N_{rm}C$ (ACY=95.0, SNY=78.0, SPY=82.0)	
					AD/MCI (ACY=96.4, SNY=76.0, SPY=85.0)	
Gerardin et al. (2009)	AD=23 $N_{rm}C$ =25 MCI=23	HCUDC	Hippocampus shape	SVM	**AD/ $N_{rm}C$** (ACY=94.0, SNY=96.0, SPY=92.0) **MCI/ $N_{rm}C$** (ACY=83.0, SNY=83.0, SPY=84.0)	Hippocampus is highly influenced by Alzheimer's disease at the initial stage. The author has used it as ROI, which holds importance. The author used a region-growing approach for segmentation which is not very efficient for segmentation due to the complex structure of the brain (Pang et al., 3 Apr. 2017). Dataset is very small.
Farhan et al. (2014)	AD=37 $N_{rm}C$ =48	OASIS	Area of the left hippocampus	Ensemble (SVM, MLP, Decision Tree)	**AD/ $N_{rm}C$** (ACY=93.8, SNY=87.5, SPY=100.0)	Dataset is very small. ROI mask is prepared by manually segmenting half of the images in the dataset. And, then coordinates of the mask are applied to the rest of the images. Manual segmentation can lead to errors (Khlif et al., 2019).
Wang et al., (2007)	AD=18 $N_{rm}C$ =26	ADRC	Hippocampus shape	LR	**AD/ $N_{rm}C$** (ACY=81.1)	Shape features suffer from the problem of high dimensionality, are noisy, and hence not reliable (Park et al., 2012)
Ben Ahmed et al. (2015)	AD=35 $N_{rm}C$ =72 MCI=111	ADNI	Hippo VF (CHF) + CSF VOLUME	SVM	**AD/ $N_{rm}C$** (ACY=87.0, SNY=100.0, SPY=75.5)	Atlas-based segmentation is used by the author for segmenting the hippocampus. The atlas-based approach lacks boundary information (Gao and Tannenbaum, 2011), which results in inaccurate ROI segmentation.
					MCI/ $N_{rm}C$ (ACY=78.2, SNY=83.3, SPY=70.7)	
					AD/MCI (ACY=72.2, SNY=70.0, SPY=75.0)	
		"Bordeaux dataset	Hippo VF (CHF) + CSF VOLUME	SVM	**AD/ $N_{rm}C$** (ACY=85.0, SNY=81.0, SPY=76.0)	

OASIS=Open access series of imaging initiative Accuracy=ACY, Sensitivity=SNY, Specificity=SPY
ADNI= Alzheimer's Disease Neuroimaging Initiative
HCUHC=Hospital Centre University De Caen, Caen, France
ADRC= Alzheimer disease research center

Qiu et al., 2008; Astrakas and Argyropoulou, 2010; Cuingnet et al., 2011).

3.2. Voxel-based morphometry (VBM)

VBM provides the voxel-wise analysis of grey matter density, white matter density, and cerebrospinal fluid in MR scans of the brain (Karas et al., 2003 Apr). This technique helps in comparing the brains of two subjects with different shapes and topologies. In VBM a spatial normalization technique is used to map the subject images on a template (Valsasina et al., 2012). VBM follows a three-step process:

- Preparation of a template from high-resolution structural MR images.
- MR images of subjects are spatially normalized, segmented into CSF, grey, and white matter according to pixel intensity, and then smoothed for compensating any structural variation during the normalization process using a consistent Gaussian kernel.
- Finally, it provides the inter-subject comparison between brains of different shapes by doing voxel-wise comparisons of grey and white matter.

VBM gives more promising results compared to ROI based approach (Davatzikos et al., 2008b). One of the limitations of VBM is to maintain the same scanning and imaging parameters for scanning all the raw images. Other potential issues related to VBM are the difficulty of spatially normalizing a typical brain, the robustness of the standard parametric test, and the interpretation of the results (Andrea Mechelli et al., 2005). VBM can be classified as a whole density map and a reduced density map.

3.2.1. Whole density map

The whole density map includes tissue density maps viz. WM, GM, or both as features. In this method, all the features are used for classification, which results in high dimensionality (Jia et al., 2022) and the problem of overfitting (Hawkins, 2004). High dimensionality occurs when the training dataset has a greater number of features compared with the number of training subjects. High dimensionality results in overfitting (Cook and Ranstam, 2016), which means that the classification model gives high and low accuracy with training and new test dataset respectively. This is because details and noise in the training data are learned by the model which has a negative impact on the performance of the model on test data. Klöppel et al. (2008) obtained GM density maps from the entire brain and used them as features. The authors observed relatively low GM density in the hippocampus of AD patients and obtained 95.6% accuracy in AD/$N_{rm}C$ classification. Möller et al. (2016) also obtained GM density maps from the whole brain for SVM-based AD/$N_{rm}C$ classification.

3.2.2. Reduced density map

In this method, the dimensions of features are reduced by selecting relevant features and removing redundant information. Supervised, unsupervised, and pre-defined atlases-based methods are used for reducing dimensions.

3.2.2.1. Unsupervised methods. The unsupervised methods do not require labelled data while learning low dimensional feature space (Ghahramani, 2003). Principal component analysis (PCA) is an unsupervised method used by researchers to reduce the dimension of white matter and grey matter features (Salvatore et al., 2015). The reduced features are then used to classify AD and to evaluate the progression of MCI (Gupta et al., 2019a). Razavi et al. (2019) used unsupervised feature learning which was composed of two stages: The first stage was scattered filtering which was applied to obtain features from images. The second stage implemented the Softmax regression for AD/ $N_{rm}C$ classification. Lama et al. (2017) achieved an improved classification accuracy from 57.6 to 59.8% for MCI/ $N_{rm}C$ /AD classification by using PCA-based feature selection and Robust Extreme Learning Machine (RELM) classifier. Baskar et al. (2019) tested both supervised and unsupervised techniques to classify Normal Control, MCI, and AD. The authors used a backpropagation artificial neural network as a supervised technique and Kernel fuzzy c-means as an unsupervised technique.

3.2.2.2. Supervised methods. Supervised methods require labelled data while learning low dimensional feature space (Vogelstein et al., 2021). Beheshti et al. (2015) in 2015 proposed a probability distribution function-based feature selection approach. It was a supervised technique that used the Fisher criterion maximization method for reducing the feature dimensions. The voxel intensity of GM maps was used as a feature for AD classification. The technique helped in achieving around 89.7% accuracy for AD/ $N_{rm}C$ classification with SVM classifier. Beheshti et al. (2017) in 2017 proposed a feature selection method based on genetic algorithm and feature ranking and achieved an improved classification accuracy up to 93.0% in AD/ $N_{rm}C$ classification. Fisher criterion had been used as the objective function in genetic algorithms. In addition to optimal feature selection, this method performed dimensionality reduction also.

3.2.2.3. Atlas-based methods. In their method, a pre-defined anatomically labelled atlas was used to parcellate the brain image into various anatomical regions, and then features were extracted from the anatomical regions (Tzourio-Mazoyer et al., 2002; Shattuck et al., 2008). Magnin et al. (2009) parcellated the brain image into 116 regions by using a labelled atlas and extracted grey matter features from parcellated regions which were further classified using Support Vector Machine (SVM) classifier. Fan et al (Fan et al., 2007a). calculated an adaptive set of ROIs by finding Regional Analysis of Volumes Examined in Normalized Space (RAVENS) density plots (Davatzikos et al., 2001) and with a watershed clustering algorithm (Ng et al., 2006). This adaptive ROI approach further reduced the feature dimensions. Depending upon the number of atlases being used, the approach can be divided into single atlas and multiple atlas methods. In a single atlas, subject images are aligned into one atlas to find the appropriate ROIs, and to extract the volumetric features from respective ROIs (Weiner et al., 2015). In multiple atlas methods, subject images are aligned into multiple atlases to find appropriate ROIs and then volumetric features are calculated from respective ROIs in each atlas space.

Fan et al. (2008a) proposed a pattern classification approach using patterns like temporal lobe, grey matter regions, peri-hippocampal white matter, and CSF and obtained an accuracy of 94.3% in AD/ $N_{rm}C$ classification. Fan et al. (2007a) proposed the Classification of Morphological Patterns using the Adaptive Local Regional Element algorithm (COMPARE) for extracting features by using a single atlas. Many researchers used this algorithm (Fan et al., 2008b, 2008a, 2007b, 2008b). Cuingnet et al. (2011) compared the performance of ten feature extraction techniques. These techniques included five voxel-based, three cortical thickness-based, and two hippocampus-based techniques. Out of these techniques, voxel-based techniques and cortical thickness-based techniques proved to be more promising. A single atlas was used in these techniques for feature extraction. Liu et al. (2012) in 2012 used a single atlas to divide the brain images into local patches for capturing spatial consistency. The group of patches was taken randomly to build a weak classifier. The final decision was then based on the combined outcome of all weak classifiers. Later in 2014, Liu et al. (2014a) proposed a hierarchical ensemble classification method for dealing with the problem of high dimensionality. The authors divided the whole brain image into a number of patches using a single atlas and obtained two different features viz. i) Grey Matter (GM) density maps from local patches, ii) spatial-correlation features based on correlations among local patches. Then two low-level classifiers were designed to convert

these features into high-level features which were further given to multiple high-level classifiers. The final decision was based on the outcome of all high-level classifiers. A single atlas (Doan et al., 2010) is generally biased toward a specific class so it may not be able to depict the minute dissimilarities between the brain of AD patients and healthy subjects and hence is unable to represent all the subjects effectively. Therefore, most of the researchers use multiple atlases.

Multiple atlases give complementary information for classification and remove the impact of registration errors. Lepore et al. (2008) used multiple atlases for image registration. The authors then averaged the information received from multiple atlases. Lepore et al. (2008) and Koikkalainen et al. (2011) used multiple atlases that were nonlinearly aligned to a common space. The problem with this method was that it lacked in considering the anatomical differences in different atlases. As a solution to this, Min et al. (2014) used Affinity Propagation Algorithm (Frey and Delbert, 2007) to select multiple atlases from the different groups of patients. These atlases were in their original spaces without confining them to a common space thus more distinctive features could be obtained from them. The drawback of this work was that the features generated from different atlases were concatenated which resulted in information redundancy. Subsequently, to resolve this, Liu et al. (2015a). in 2015 proposed a View centralised multi-atlas classification method in which the authors kept all the atlases in their original space and extracted features from individual atlas only along with the complimentary feature information obtained from other atlases. SVM was used in ensemble mode in this work.

Liu et al. (2016a) in 2016 observed how the multiple atlases and how the patients within the same atlas are related to each other. The authors then proposed the Relationship Induced Sparse Feature Selection method (RISFS) in which they registered the image onto multiple atlases and extracted unbiased features in each atlas space. Liu et al. (2016b) in 2016 also proposed a new technique for feature selection that was based on the structural details of different patients related to the same class. Based on these structural details, the class may be divided into subclasses that can be encoded and used for classification.

Techniques other than VBM are Deformation-Based Morphometry (DBM), Landmark-Based Morphometry (LBM), and Tensor-Based Morphometry (TBM). DBM focuses on the positional difference of every voxel to a normal brain whereas TBM uses the gradient of deformation to either register each subject's MR scan to a template (cross sectional studies) or to register each subject's follow-up scan to their baseline scan (longitudinal studies) (Ashburner and Friston, 2000; Ashburner et al., 1998; Teipel et al., 2007). VBM and DBM approaches use nonlinear image-alignment to templates (Khan et al., 2015). One of the drawbacks is – that due to the high anatomical variability of brain structures, these techniques lose the accuracy of image alignment from patient to patient. Another risk is around misalignment (Bookstein, 2001) or an over-alignment that may result in the loss of informative patterns from the images (Toews et al., 2010). In LBM a group comparison is performed based on local morphological features to identify brain regions that are more prone to differences. The centers of these identified regions become landmarks. This method does not use nonlinear registration or tissue segmentation like VBM / DBM. Zhang et al. (2017) demonstrated the importance of the LBM technique over VBM / DBM / TBM. Table 2 lists prominent studies for the AD classification framework using voxel-based methods.

Table 2 indicates the different approaches for dimensionality reduction. The unsupervised technique for dimensionality reduction has the disadvantage that it does not explore spatial information from images (Lin et al., 2015). The single atlas-based approach is generally biased towards a specific group of classes and thus does not provide accurate results (Doan et al., 2010). Recently researchers are focusing on multiple atlas-based approaches as these are not biased to specific classes and can even explore the subcategories within a class (Liu et al., 2016b).

3.3. Cortical surface-based methods

Structural changes at the cortical surface are striking especially in temporal and parietal regions due to Alzheimer's disease (Bakkour et al., 2009; Dickerson et al., 2009a). Cortical thinning (Singh et al., 2006; Du et al., 2007), sulcal widening (Liu et al., 2013a), reduction in cortical thickness (Dickerson et al., 2009b; Long et al., 2013), and mean curvature in the temporal lobe (Im et al., 2008) are the main structural changes in the brain of MCI patients as compared with normal controls. The cortical thickness is computed by measuring the distance between the white and pial surfaces at each vertex of the cortical surface (Hutton et al., 2008; Clarkson et al., 2011). In recent research, cortical features related to cortical thickness, curvature, sulcal depth that shows the degree of cortical folding, gyrification index (Armstrong Armstrong et al., 1995; Zilles et al., 1988) that measures surface complexity, and surface area that shows the total area of the surface across a brain region have been extracted through surface-based morphometry using the Freesurfer toolbox (Clarkson et al., 2011). Surface-Based Morphometry (SBM) is a morphometric technique used for the structural analysis of the brain (Ghosh et al., 2010). This technique helps in assessing the structural variation of the cortical surface with the progression of the disease (Libero et al., 2014). Cortical features obtained from vertices can be used directly or can be used after reducing their dimensions. Thus, there are two methods i) directly used features methods, and ii) reduced features dimension-based methods.

3.3.1. Directly used features methods

This method utilizes all the features extracted from each vertex of the cortical surface. Li et al. (2014) used a multivariate computational approach by combining six cortical features. These features were cortical surface area, cortical thickness, sulcal depth, GM volume, metric distortion, and cortical curvature extracted from all vertices of the pial surface. The authors used all these features to analyze the grey matter distribution in stable MCI and observed that all these cortical features were useful in discriminating normal controls from stable MCI patients. The features extracted from the right hemisphere and left hemisphere yielded 80.0% and 76.0% accuracy respectively. The directly used feature methods suffer from the problem of high dimensionality.

3.3.2. Reduced features dimension-based methods

This method solves the problem of high dimensionality. In this method instead of using all the features from the cortical surface, only relevant features are used. These relevant features are obtained from the region of pre-defined atlas or by using supervised and unsupervised techniques for feature dimension reduction.

3.3.2.1. Unsupervised/Supervised feature reduction-based method. Gupta et al. (2019b) extracted cortical thickness and subcortical volume as features using Freesurfer. The authors used PCA for reducing feature dimensions and obtained an accuracy of 99.3% in AD/ $N_{rm}C$ classification with a softmax classifier. Cho et al. (2012) converted cortical thickness data into their spatial frequency components through manifold harmonic transform. The authors used Linear Discriminant Analysis (LDA) for reducing feature dimensions by removing high-frequency (noise) components and obtained sensitivity of 82.0%, and specificity of 93.0% for AD/ $N_{rm}C$ classification, sensitivity of 66.0%, and specificity of 89.0% for $N_{rm}C$ /pMCI classification, sensitivity of 63.0%, and specificity of 76.0% for sMCI/pMCI classification. Park et al. (2012). in 2012 used cortical thickness and sulcal depth as features. The authors reduced feature dimensions by PCA and obtained 90.0% accuracy in AD/ $N_{rm}C$ classification with SVM classifier. Park et al. (2013) in 2013 implemented the same classification framework to longitudinal MRI data and achieved 83.0% accuracy in AD/MCI classification.

3.3.2.2. Atlas-based methods. These methods include the tessellation of

Table 2
Performance comparison of prominent studies for AD classification with $N_{rm}C$ and MCI using voxel-based methods.

Author	Data Set	Method	Database	Feature Type	Classifier	Performance	Observations
Salvatore et al. (2015)	AD=137 $N_{rm}C$ =162 sMCI=134 pMCI=76	Unsupervised (PCA)	ADNI	Voxel Wise	SVM	**AD/ $N_{rm}C$** (ACY=76.0)	PCA is used for dimensionality reduction. PCA causes spatial loss of information (Lin et al., 2015)
						pMCI /sMCI (ACY=66.0)	
						MCI / $N_{rm}C$ (ACY=72.0)	
Gupta et al. (2019a)	AD=81 $N_{rm}C$ =171 sMCI=35 pMCI=39	Unsupervised (PCA)	NRCD	Hippocampal Volume, Voxel-Based Morphometry, Cortical and Subcortical segmented region	k-NN	**AD / $N_{rm}C$** (ACY=89.4, SNY=93.8, SPY=88.3)	PCA is used for dimensionality reduction. PCA causes spatial loss of information (Lin et al., 2015)
						pMCI / sMCI (ACY=73.9, SNY=70.6, SPY=83.3)	
						MCI / $N_{rm}C$ (ACY=88.9, SNY=94.1)	
					RF	**AD / $N_{rm}C$** (ACY=88.2, SNY=78.3, SPY=92.5)	
						pMCI / sMCI (ACY=78.3, SNY=76.9, SPY=80.0)	
						MCI / $N_{rm}C$ (ACY=87.3, SNY=93.9)	
					SVM	**AD / $N_{rm}C$** (ACY=93.1, SNY=87.9, SPY=95.6)	
						pMCI / sMCI (ACY=86.9, SNY=77.8, SPY=92.8)	
						MCI / $N_{rm}C$ (ACY=95.2, SNY=95.8)	
Beheshti et al. (2015)	AD=130 $N_{rm}C$ =130	Supervised (Probability distribution function)	ADNI	Voxel wise	Linear SVM	**AD / $N_{rm}C$** (ACY=89.7, SNY=87.7, SPY=91.6)	DARTEL registration technique is used by the author for image registration which has a limitation that by using this it is impossible to get large deformations for which velocities do not remain constant (Ashburner, 2007). The partial Least Squares (PLS) method is used for feature extraction which has the drawback that it overrates and extracts irrelevant features (Pirouz, 2006).
Beheshti et al. (2017)	AD=160 $N_{rm}C$ =160 sMCI=65 pMCI=71	Supervised (test +GA)	ADNI	Voxel wise	SVM	**AD / $N_{rm}C$** (ACY=93.0, SNY=89.1, SPY=96.8)	The t-Test method is used for feature selection, which is more prone to Type I error, which means it may cause inaccurate results when the variances are not combined positively (Nor Aishah Ahad and Sharipah Soaad Syed Yahaya, 2014).
						pMCI / sMCI (ACY=75.0, SNY=76.9, SPY=73.2)	
Cuingnet et al. (2011)	AD=137 $N_{rm}C$ =162 sMCI=134 pMCI=76	Single atlas	ADNI	Voxel-Direct-D GM	SVM	**AD / $N_{rm}C$** (ACY=88.6, SNY=81.0,	A single atlas generally represents a specific group of classes (Doan et al., 2010).

(*continued on next page*)

Table 2 (*continued*)

Author	Data Set	Method	Database	Feature Type	Classifier	Performance	Observations
						SPY=95.0) **pMCI / sMCI** (ACY=70.4, SNY=57.0, SPY=78.0) **MCI / $N_{rm}C$** (ACY=81.1, SNY=73.0)	
Liu et al. (2012)	AD=198 $N_{rm}C$ =229 MCI=225	Single atlas	ADNI	Voxel-Wise GM	SRC ensemble	**AD / $N_{rm}C$** (ACY=90.8, SNY=86.3, SPY=94.8) **MCI / $N_{rm}C$** (ACY=87.8, SNY=85.3)	A single atlas generally represents a specific group of classes (Doan et al., 2010).
Liu et al. (2014a)	AD=198 $N_{rm}C$ =229 MCI=225	Single atlas	ADNI	Patch-Based GM	SVM ensemble	**AD / $N_{rm}C$** (ACY=92.0, SNY=91.0, SPY=93.0) **MCI / $N_{rm}C$** (ACY=85.3, SNY=82.3)	The t-Test method is used for feature selection, which is more prone to Type I error, which means it may cause inaccurate results when the variances are not combined positively (Nor Aishah Ahad and Sharipah Soaad Syed Yahaya, 2014).
Koikkalainen et al. (2011)	AD=88 $N_{rm}C$ =115 sMCI=115 pMCI=54	Multi atlas	ADNI	Tensor-Based Morphometry	Linear regression	**AD / $N_{rm}C$** (ACY=86.0, SNY=81.0, SPY=91.0) **pMCI / sMCI** (ACY=72.1, SNY=77.0, SPY=71.0)	Multiatlas methods have reduced the negative impact of registration errors. The drawback is that the multiple atlases used for registration were nonlinearly aligned to common space thus morphometric patterns generated by them would be less informative (Lepore et al., 2008).
Min et al. (2014)	AD=97 $N_{rm}C$ =128 sMCI=117 pMCI=117	Multi atlas	ADNI	Data driven ROI GM	SVM	**AD / $N_{rm}C$** (ACY=91.6, SNY=88.6, SPY=93.8) **pMCI / sMCI** (ACY=72.4, SNY=72.1, SPY=72.6)	The authors used the Affinity Propagation algorithm for selecting multiple atlases (Li et al., 2009) and atlases are not confined to a common space.
Liu et al. (2015a)	AD=97 $N_{rm}C$ =128 sMCI=117 pMCI=117	Multi atlas	ADNI	Data-driven ROI GM	SVM ensemble	**AD / $N_{rm}C$** (ACY=92.5, SNY=92.9, SPY=88.3) **pMCI / sMCI** (ACY=78.9, SNY=85.4, SPY=76.1)	Multi atlas-based image registration technique is used which is computationally expensive (Bjoern Menze et al., 2014). Longitudinal discriminative information is not considered in this paper which may be helpful for AD classification (Yesavage and Brooks, 1991).

SRC= Sparse representation-based classifier Accuracy=ACY, Sensitivity=SNY, Specificity=SPY
SVM=Support vector machine
k-NN=Nearest Neighbor classifier
RF=Random Forest
NRCD=National Research Center for Dementia

regions in the brain using certain standardized atlases (Fischl et al., 1999). Cortical features are then extracted from these tessellated regions (Fischl and Dale, 2000; Jones et al., 2000; MacDonald et al., 2000; Desikan et al., 2006; Ye et al., 20082008; Querbes et al., 2009). Desikan et al (Desikan et al., 2009). obtained cortex thickness and hippocampal volume features from 34 neuroanatomic regions of the brain. These regions included 32 gyral-based ROIs from the neocortex, plus the amygdala and hippocampus. This study showed the importance of examining the supramarginal gyrus for differentiating MCI from AD. Oliveira et al. (2010) extracted cortical thickness features from several specific regions by using atlases and the mean cortical thickness features from the whole brain. The authors used SVM for AD/ $N_{rm}C$ classification and obtained more promising results with the mean cortical thickness features extracted from the whole brain. Wee et al. (2013) demonstrated significant improvement in the classification results by using correlative morphological information. They extracted different cortical morphological information such as thickness measures from specific regions, GM and WM volumes from the cerebral cortex, and correlated features because different regions of the brain have correlated cortical thickness. Eskildsen et al. (2013) examined the atrophy pattern of cortical thickness by avoiding double-dipping (Kriegeskorte et al., 2009) and obtained an accurate estimate of the predictive power of cortical thickness

measurement. Double dipping occurs due to the inclusion of test subjects while calculating the statistical maps. The authors obtained an accuracy, sensitivity, and specificity of 80.9%, 78.7%, and 82.8% respectively with sMCI vs pMCI6 (pMCI6 refer MCI patients progress to AD in 6 months), 74.5%, 75.2%, and 73.9% respectively with sMCI vs pMCI12 (pMCI12 refer MCI patients progress to AD in 12 months), 77.3%, 69.0%, and 79.1% respectively with sMCI vs pMCI36 (pMCI36 refer MCI patients progress to AD in 36 months) and 86.7%, 80.4%, and 92.0% respectively with MCI vs $N_{rm}C$. Table 3 lists prominent studies for AD classification framework using cortical surface or vertex-based methods.

Table 3 indicates different approaches for reducing the dimensions of features obtained from the cortical surface. Generally, authors have used PCA for reducing the dimensions of features. PCA has limitations in that it supports gaussian data and is scale-invariant in nature (Han and Liu, 2013). Atlas-based methods require the selection of a proper atlas and proper alignment of images over atlases (Yeo et al., 2008).

3.4. Wavelet transform- based method

Wavelet Transform is the most common approach for extracting localized frequency information from a signal (Moulin, 2009; Zhang, 2019). This approach can find the finest details in an image. Wavelet transform captures the high-frequency variation in grey level concentration (Lahmiri and Boukadoum, 2013; Davatzikos et al., 2003). Imaginary coefficients in complex wavelets provide the edge information thus becoming an important approach for AD diagnosis. Wavelet transform has directional selectivity thus providing features in different directions. This method is also beneficial in providing the whole-brain analysis. Voxel-based methods and vertices-based methods for feature extraction come under whole-brain analysis and these methods provide better classification results in comparison to ROI-based methods (Cuingnet et al., 2011).

In more advanced stages of AD, atrophy expands from a single region to multiple regions. Thus, segmentation of the brain region is not required as it is required in the case of ROI-based approaches. More importantly, the whole-brain analysis considers the entire brain as a single ROI. This whole-brain analysis includes two stages i.e., feature extraction and classification. It requires however the scanning of all voxels of the brain and thus suffers from feature dimensionality problems (Wachinger et al., 2016; Liu et al., 2018).

Some researchers used wavelet coefficients directly as features while others generate texture features through wavelet coefficients. Texture features include mean, variance, wavelet energy, entropy, contrast, and homogeneity. El-Dahshan et al. (2010) applied Discrete Wavelet Transform (DWT) on 2-D MR images and used 3rd level detail to approximate wavelet coefficients as features. The authors used PCA for feature dimension reduction and achieved 97.0% accuracy with Feed-forward Artificial Neural Network classifier and 98.0% accuracy with

Table 3
Performance comparison of prominent studies for AD classification with $N_{rm}C$ and MCI using cortical surface or vertex-based methods.

AUTHOR	DATA SET	Database	Feature Type	Classifier	Performance	Observations
Li et al. (2014)	MCI=24 $N_{rm}C$ =26	Xuan Wu Hospital (CHINA)	All vertices (right hemisphere)	SVM	**sMCI / $N_{rm}C$** (ACY=80.0)	It is a multivariate approach. Dataset size is small which influences the performance of the classifier negatively (Hua et al., 2005).
Gupta et al., (2019b)	AD=81 $N_{rm}C$ =171 pMCI=39 sMCI=35	NRCD	Reduced vertices	Softmax	**AD / $N_{rm}C$** (ACY=99.3)	The author used the Freesurfer toolbox for cortical thickness measurement. FreeSurfer has a drawback that it shows biases at the time of measurement. These biases may require statistical adjustments (Schmidt et al., 2018).
				SVM	**AD / $N_{rm}C$** (ACY=98.0, SNY=97.9, SPY=98.1)	
					pMCI / sMCI (ACY=97.8, SNY=100.0, SPY=95.2)	
					pMCI / $N_{rm}C$ (ACY=99.2, SNY=99.0, SPY=100.0)	
Cho et al., (2012)	AD=128 $N_{rm}C$ =160 pMCI=72 sMCI=131	ADNI	Reduced Vertices	LDA	**AD / $N_{rm}C$** (ACY=88.3, SNY=82.0, SPY=93.0)	PCA is used for feature dimension reduction which requires the dataset to be gaussian in nature (Han and Liu, 2013). The common template is used for all subjects which should not be biased towards a specific class. Noise is removed from cortical thickness by removing high-frequency components.
					pMCI / sMCI (ACY=71.2, SNY=63.0, SPY=76.0)	
					pMCI / $N_{rm}C$ (ACY=82.0, SNY=66.0, SPY=89.0)	
Park et al. (2012)	AD=25 MCI=25 $N_{rm}C$ =50	OASIS	Reduced Vertices	SVM	**AD / $N_{rm}C$** (ACY=90.0)	PCA is used for dimension reduction which has its limitation of being scale-invariant (Han and Liu, 2013). Sulcal depth is introduced as a new feature as it is good for the classification of AD/MCI.
					pMCI / $N_{rm}C$ (ACY=86.0)	
					AD / MCI(ACY=90.0)	
Park et al. (2013)	MCI=30 pMCI=12 $N_{rm}C$ =30	ADNI	Reduced Vertices	SVM	**pMCI / $N_{rm}C$** (ACY=90.0)	PCA is used for dimension reduction which has its limitation of being scale-invariant (Han and Liu, 2013). The author used longitudinal studies which are good for AD prediction.
					AD / MCI(ACY=83.0)	

LDA = Linear Discriminant Analysis
Accuracy=ACY, Sensitivity=SNY, Specificity=SPY

k-Nearest Neighbor classifier(k-NN). DWT extracts features in only four directions viz. horizontal, vertical, and diagonal. DWT does not give phase information and is highly phase sensitive. As a solution to this Jha et al. (2017) applied Dual-Tree Complex Wavelet Transform (DTCWT) (Kingsbury, 2001) which extracts features in six different directions, viz. ±15°,±45°,±75° and provides real and imaginary wavelet coefficients. The authors extracted 32 2-D center slices from 3-D MRI and obtained detail coefficients at the 5th scale of decomposition by applying DTCWT. PCA was used for reducing feature dimensions and the accuracy achieved was 90.1% in AD/ $N_{rm}C$ classification with Feed Forward Neural Network. Alam et al. (2017) improved this work by using Linear Discriminant Analysis (LDA) with PCA, and Twin Support Vector Machine (TSVM) and obtained an accuracy of 92.7 ± 1.2% using the Alzheimer's Disease Neuroimaging Initiative (ADNI) dataset. Jha et al. (2018) used an Extreme learning machine (ELM) classifier in place of TSVM with PCA and LDA and obtained 90.3 ± 1.2% accuracy with the ADNI dataset and 95.7 ± 1.5% accuracy with the Open Access Series of Imaging Studies (OASIS) dataset. Jha et al (Jha and Kwon, 2018). worked with contourlet transform to obtain features from 2-D MR images and obtained 91.1% accuracy with an ensemble classifier (RUS Boosted Trees). Acharya et al. (2019). used Shearlet transform with k-NN Classifier for AD classification and obtained 98.5% accuracy for 2-D MR images.

Some authors also worked on 3-D MR images. Bhasin et al. (2020) used 3-D-DWT and LBP-20 for extracting features and obtained 90.3% accuracy in MCI/ $N_{rm}C$ classification. LBP is an important feature extraction technique used to obtain statistical and morphological information from the image dataset (Ojala et al., 1996). It helps in capturing the details related to various microstructures like edges etc. LBP also solves the problem of high dimensionality (Ojala et al., 2002). Zhang et al. (2015) used 3-D DWT to obtain coefficients from the 3-D MR image and further used these coefficients to generate features such as energy, variance, and Shannon entropy. Garg and Chaudhary (2021) applied DTCWT for extracting mean energy features and achieved the maximum accuracy of 97.5% The corresponding feature vector consisted of the mean energy of real coefficients and mean energy of imaginary coefficients. Table 4 lists the prominent studies for the AD classification framework using wavelet transform-based method.

Table 4 indicates that wavelet coefficients are promising features for AD classification. Generally, PCA has been used by the authors for reducing feature dimensions that cause spatial loss of information (Abdi and Lynne, 2010). The wavelet has directional sensitivity and can extract features in different directions. For instance, DWT can extract features in four directions (Jha et al., 2017; Alam et al., 2017) and DTCWT can extract features in six different directions. The Wavelet Transform approach for feature extraction suffers from high dimensionality as features are extracted from the whole brain (Wachinger et al., 2016; Liu et al., 2018).

3.5. Texture-based methods

Texture-based feature extraction techniques provide distinguishing features from the brain which is very helpful for identifying AD and MCI. Texture provides information regarding shape, density, pixel value, etc. in an image by capturing local variation in intensity at consistent intervals (Alobaidli et al., 2014). The texture is of two types, one is structural which includes Local Binary Pattern (LBP), Fourier coefficients, wavelet coefficients and another one is statistical which includes a histogram, Grey-Level Co-occurrence Matrix (GLCM), and Grey Level Run Length Matrix (GLRLM). GLCM and GLRLM are matrices that provide textural features for texture analysis. GLCM (Chen and Feng Yu Yang, 2012) is a matrix whose elements represent how often the distinct sets of pixel grey level intensity repeat in an image. The GLRLM (Dash and Manas Ranjan Senapati, 2021) is a matrix that determines the count of grey level runs of various run lengths. A grey level run represents the line of pixels in a definite direction having identical intensity values, the grey level run length represents the count of corresponding pixels, and the run-length value represents the count of incidents. Out of these textural features, GLCM has proved to be the best and has been commonly used by researchers (Larry, 1975; De-Shuang Huang et al., 2008). Haralick et al. (1973) obtained the texture features with the GLCM and some of these features with their equations are given in Table 5 (Haralick et al., 1973; Barburiceanu et al., 2021).

Several researchers are using 3-D Texture Analysis as these

Table 4
Performance comparison of prominent studies for AD classification with $N_{rm}C$ and MCI using wavelet transform based method.

AUTHOR	Feature extraction	DATABASE	Data set	Classifier	Performance	Observations
Jha et al. (2017)	DTCWT+ PCA	OASIS	AD=28 $N_{rm}C$ =98	FNN	**AD / $N_{rm}C$** (ACY=90.1, SNY=92.0, SPY=87.8)	1. Authors have extracted 32 2-D slices from 3-D MRI which is done manually and requires expert knowledge. 2. PCA is used for feature reduction which causes spatial loss of information (Abdi and Lynne, 2010).
Alam et al. (2017)	DTCWT+ PCA + TSVM+LDA	OASIS	$N_{rm}C$ =44 AD=51	TSVM	**AD / $N_{rm}C$** (ACY=96.7, SNY=97.7, SPY=95.6)	1. Authors have extracted 32 2-D slices from 3-D MRI which is done manually and requires expert knowledge.
		ADNI	$N_{rm}C$ =86 AD=86	TSVM	**AD / $N_{rm}C$** (ACY=92.7, SNY=93.1, SPY=92.2)	2. PCA is used for feature reduction which causes spatial loss of information (Abdi and Lynne, 2010).
Bhasin et al. (2020)	3-D DWT+LBP20	ADNI	sMCI=112 pMCI=75 $N_{rm}C$ =89	SVM	**pMCI / sMCI** (ACY=88.7, SNY=90.2, SPY=89.2) **MCI vs $N_{rm}C$** (ACY=90.3, SNY=90.2, SPY=90.2)	1.DWT is used for feature extraction which extracts features from four directions only (Jha et al., 2017; Alam et al., 2017) which are not more informative.
Acharya et al. (2019)	ST	Clinical Brain MRI Dataset	$N_{rm}C$ =110 AD=55	k-NN	**AD / $N_{rm}C$** (ACY=98.5, SNY=96.9, SPY=100.0)	1. The t-Test method is used for feature selection, which is more prone to Type I error (Nor Aishah Ahad and Sharipah Soaad Syed Yahaya, 2014). 2. The k-NN classifier is used which faces difficulty in finding the optimum value of k (Abu Alfeilat et al., 2019 Dec). A k-NN is a lazy learner as learning is based on distance measurement between the neighbors (Parvin et al., 2008).

FNN = Feed-Forward Neural Network
TSVM = Twin Support Vector Machine
ST = Shearlet Transform
Accuracy=ACY, Sensitivity=SNY, Specificity=SPY

Table 5
GLCM features with equations.

S.No	Features	Formula	Notation
1	Autocorrelation	$F_1 = \sum_{j}^{N}\sum_{k}^{N} jkW_{jk}$	
2	Contrast	$F_2 = \sum_{n=0}^{N-1} n^2 \left\{ \sum_{k}^{N} W_{jk} \right\}$	N= number of grey levels j= row number k= column number
3	Correlation	$F_3 = \sum_{j}^{N}\sum_{k}^{N} \frac{jkW_{jk} - \pi_x\mu_y}{\sigma_x\sigma_y}$	π_x= mean of P_x μ_y= mean of P_y
4	Cluster Prominence	$F_4 = \sum_j^N \sum_k^N W_{jk}\left(j + k - \pi_i\mu_j\right)^4$	σ_x=standard deviation of P_x σ_y= standard deviation of P_y P_x and P_y are partial probability density functions.
5	Cluster shade	$F_5 = \sum_j^N \sum_k^N W_{jk}\left(j + k - \pi_x\mu_{jy}\right)^3$	
6	Dissimilarity	$F_6 = \sum_j^N \sum_k^N \lvert j-k\rvert$	
7	Energy	$F_7 = \sum_j^N \sum_k^N {W_{jk}}^2$	W_{jk}= element j,k of the normalized symmetric GLCM.
8	Entropy	$F_8 = \sum_j^m \sum_k^n W_{jk} log(W_{jk})$	n=amount of paired data
9	Homogeneity	$F_8 = \sum_j^m \sum_k^n \frac{W_{jk}}{1+\lvert j-k\rvert}$	μ=GLCM mean
10	Maximum Probability	$F_{10} = \max_{j,k} W_{jk}$	
11	Variance	$F_{11} = \sum_j^N \sum_k^N (j-\pi)^2 W_{jk}$	σ= variance of pixel intensity contributing to GLCM
12	Sum average	$F_{12} = \sum_{n=2}^{N} nW_{x+y,n}$	Where x and y denote the row and column entry of GLCM
13	Sum variance	$F_{13} = \sum_{n=2}^{2N} (nF_{14})^2 W_{x+y,n}$	W_{x+y} is the probability of co-occurrence matrix with co-ordinates equivalent to $_{x+y}$
14	Sum Entropy	$F_{14} = \sum_{n=2}^{2N} W_{x+y,n} log(W_{x+y,n})$	
15	Difference Variance	$F_{15} = Var(W_{x-y})$	
16	Difference entropy	$F_{16} = \sum_{n=0}^{N-1} W_{x-y,n} log(W_{x-y,n})$	
17	Information measure of correlation1	$F_{17} = \frac{F_8 - HXY_1}{max\{HX, HY\}}$	HX and HY are entropies of Wx and W_y
18	Information measure of correlation2	$F_{18} = \left[1 - e^{-2(HXY_2 - F_9)}\right]\frac{1}{2}$	
19	Inverse difference	$F_{19} = \sum \frac{W_{jk}}{1+(j-k)^2}$	
20	Inverse difference moment normalized	$F_{20} = \sum_j^N \sum_k^N \frac{W_{jk}}{1+(j-k)}$	

techniques provide more spatial resolution and higher sensitivity and specificity than 2-D techniques (Zhang et al., 2012; Kovalev et al., 2001). Simões et al. (2014) investigated the brain regions that are affected at the beginning of AD. The authors extracted 3-D texture features viz. LBP-TOP (Three Orthogonal Projections) from the specified local regions in a 3-D MR image. LBP-TOP calculates the LBP histogram at axial, coronal, and sagittal planes in the brain. This study concluded that the hippocampus and amygdala are affected in the initial phase of AD and that broader brain regions are affected as the disease progresses.

Feng et al. (2018) obtained textural features through GLCM, GLRLM, and intensity features from 116 patients and observed the right hippocampus to be the most affected part in AD. This study showed the importance of textural features for AD analysis. The textural features included uniformity, mad, kurtosis, entropy, energy, root mean square, standard deviation, skewness as intensity features, high grey level emphasis, grey level non-uniformity, low grey level emphasis, low grey level run emphasis, high grey level run emphasis as GLRLM and sum entropy, cluster tendency, correlation, cluster prominence, entropy, energy, inverse difference moment normalized, sum average, contrast, maximum probability, cluster shade, homogeneity1, homogeneity2 as GLCM. Similarly, De Oliveira et al. (2011) obtained GLCM textural features from the right and left thalamus and observed significant differences in texture for different stages of AD and normal controls. More significant differences in texture were observed on the right thalamus showing the early sign of AD progression. Gao et al. (2018) used contourlet transform and GLCM to obtain textural features from the hippocampus of 299 subjects. The authors observed that the multivariant model including textural features provided better classification results in comparison to one that excluded textural features. Salunkhe et al. (2021) used GLCM to extract textural features from the hippocampus to detect the minor changes occurring in it due to AD. Xiao et al. (2017) used the Gabor filter along with the GLCM to extract features. The authors used the SVM-recursive feature elimination method for feature selection. Tooba Altaf et al. (2017) used GLCM to obtain texture features such as color, and edge from MR images, and clinical manifestations viz. Neuropsychiatric Inventory (NPI), Functional Activities Questionnaire (FAQ), and Geriatric Depression Scale (GDS) from the segmented Grey Matter (GM), White Matter (WM), and Cerebrospinal Fluid (CSF). GLCM has the advantage that a spatial relationship exists between the co-occurring sets of pixels in different directions. This is with respect to the angular spatial relationships and distance while selecting two pixels at a time. As a result, the different grey level combinations and their positions are revealed evidently (De Siqueira et al., 2013). GLCM has the drawback of being computationally expensive. GLCM has many elements with zero value, which are irrelevant and demands high computation power (Pham, 2010). Table 6 depicts the prominent studies for the AD classification framework using Texture-based Methods.

Table 6 lists the studies that used texture features for AD classification. Proper segmentation is required to obtain texture features from the region of interest (Kalinic, 2009; Szczypiński et al., 2009). Discretization of image intensities and acquisition parameters play an important role in texture feature extraction. If it is not done properly, it leads to Magnetic Resonance Texture Analysis (MRTA) heterogeneity (Cai et al., 2020). Table 7 lists the advantages and disadvantages of different feature extraction methods discussed in this paper.

Table 7 indicates the strengths and weaknesses of feature extraction methods. The ROI technique is good for early AD detection. VBM examines the group differences and the volume of grey matter and white

Table 6
Performance comparison of prominent studies for AD classification with $N_{rm}C$ and MCI using Texture-based method.

AUTHOR	Feature extraction	DATA SET	Classifier	Performance	Observations
Simões et al. (2014)	LBP TOP from the Whole-brain	$N_{rm}C$ =66 AD=70	SVM	This study focuses on finding the most discriminative regions in early AD by analyzing LBP patches	LBP-TOP is good for edge detection. In this study, LBP-TOP is extracted from the whole brain which does not require segmentation, prior knowledge, and alignment to the template (Wang et al., 2014).
Feng et al. (2018)	Histogram, GLCM, Wavelet, GLRLM from the hippocampus	$N_{rm}C$ =45 AD=38s MCI=33	SVM	**AD / $N_{rm}C$** (ACY=86.7, SNY=84.2, SPY=88.9) **sMCI / $N_{rm}C$** (ACY=70.5, SNY=57.6, SPY=80.0) **sMCI / AD** ACY=59.1, SNY=54.5, SPY=63.2)	Hippocampus is segmented into sub-regions using atlases. Due to this, identical shape features are observed in different subregions which are not included in the study. Radiomic features viz., intensity features, and texture features of GLCM and GLRLM, are difficult to extract from subregions of the hippocampus due to atlas-based segmentation (Kalinic, 2009).
De Oliveira et al. (2011)	GLCM from Thalamus	$N_{rm}C$ =16 AD=16s MCI=17		Texture features obtained from the Corpus Callosum, and thalamus manifested distinction among AD/ $N_{rm}C$, sMCI/AD, and sMCI/ $N_{rm}C$.	Mazda software is used for the extraction of texture features which requires manual segmentation (Szczypiński et al., 2009) Manual segmentation process is time-consuming.
Gao et al. (2018)	Contourlet-based transform GLCM from hippocampus	$N_{rm}C$ =7 sMCI=73 pMCI=62	Gaussian process models Partial least squares	**pMCI / $N_{rm}C$** (ACY=86.7) **sMCI / $N_{rm}C$** (ACY=79.5) **MCI to $N_{rm}C$** (ACY=85.7)**pMCI / $N_{rm}C$** (ACY=85.5) **sMCI / $N_{rm}C$** (ACY=83.6) **MCI to $N_{rm}C$** (ACY=100.0)	Dataset is small. Texture features are obtained from the hippocampus only. Texture features obtained from other regions may improve accuracy (Chaddad et al., 2017).

Accuracy=ACY, Sensitivity=SNY, Specificity=SPY

matter at the voxel level and allows the researchers to investigate the impact of the genetic constitution, aging, gender, and developmental diseases on brain structure (Testa et al., 2004). VBM can detect small changes in grey matter while ROI can detect moderate to severe grey matter abnormalities (Seyedi et al., 2020). VBM requires the perfect registration of images on the template. VBM technique focuses on volume registration while the cortical surface-based method focuses on surface registration which is better than volume registration (Anticevic et al., 2008; Desai et al., 2005). The wavelet-based approach covers the whole brain and does not need segmentation. The only problem lies with the high dimensionality which can be solved by using feature dimension reduction methods and high-speed computers (Alvarez et al., 2009).

4. Classification methods

Classification means identifying the class of unseen input data. A classifier is a machine learning algorithm used to sort input data into labelled classes (Ayodele, 2010). This process (Lao et al., 2004) needs two sets of data, one which is used to train the classifier and the other that is to be tested. AD classification deals with the categorization of input data either belonging to the AD class, MCI class, or $N_{rm}C$ class. The training image set includes the MR images of healthy subjects and AD patients at different stages of the disease and the test image set includes MR images that are yet to be diagnosed as Normal or AD. Machine learning techniques extract features from the given MR test image and based on these features, classification among different groups is performed (Fan et al., 2005). These features are either extracted from the whole brain or any atrophied region of the brain (Camara-Rey et al., 2006) (Klöppel et al., 2008). The performance parameters of machine learning algorithms considered in almost all the studies include accuracy (Wilson, 1995), sensitivity (Ng and Jamil, 2014), and specificity (Trevethan, 2017). Accuracy indicates the ratio of data that is accurately classified by a classifier. The sensitivity indicates the ratio of true positives that are classified correctly, and specificity indicates the measure of the ratio of true negatives which are correctly classified.

$$\text{Accuracy}=(T_{pos}+T_{Neg})/(T_{pos}+T_{Neg}+F_{pos}+F_{Neg}) \quad (1)$$

$$\text{Senstivity}=T_{pos}/(T_{pos}+F_{Neg}) \quad (2)$$

$$\text{Specificity}=T_{Neg}/(T_{Neg}+F_{pos}) \quad (3)$$

T_{pos} means True positive. It shows that a person suffering from AD is rightly diagnosed. T_{Neg} means True negative. It shows that a person not suffering from AD is rightly classified as a normal person. F_{pos}means False positive. It shows that a person not suffering from AD is classified under AD. F_{Neg} means False negative. It shows that a person suffering from AD is erroneously classified as a normal person. Different machine learning algorithms have been used in Literature for classification. This review paper includes studies related to classifiers: Artificial Neural Network (ANN), Random Forest (RF), *k*-Nearest Neighbor (k-NN), Support Vector Machine (SVM), Extreme Learning Machine (ELM), and Naive Bayes (NB).

4.1. Support vector machines (SVM)

Particularly SVM has been extensively used for the classification of AD subjects from normal controls by using structural MRI (Klöppel et al., 2008), (Vemuri et al., 2008). SVM draws the hyperplane between the training samples of both classes and selects the best hyperplane which maximizes the margin between the samples of both classes. SVM can be used with different kernels in classification frameworks. Most researchers have used linear SVM to distinguish AD from $N_{rm}C$, as there is no need of tuning kernel parameters in linear SVM. Few studies also deal with multiple kernels for SVM (Saruar Alam, 2017). Multiple kernel learning methods use a set of different kernels. This method is preferable when data is to be combined from different sources. A learning method is there to pick the best kernel or the combination of kernels. Single kernel generally becomes a source of biased information (Liu et al., 2014a). Klöppel et al. (2008) classified the clinically approved AD patients and Normal elderly controls through linear SVM. The authors analyzed the concentration of grey matter in T1-weighted MR scans. Khedher et al. (2017) observed that linear kernel yields high classification accuracy of 89.0% for large dimensional data in contrast with polynomial kernel. Nevertheless, some studies include the usage of polynomial kernel. Lahmiri and Boukadoum (2014) observed good accuracy in multiclass classification of $N_{rm}C$, MCI, and AD using polynomial kernel. Zhang et al. (2015) achieved an accuracy of 92.4% using PCA with polynomial kernel.

4.2. Random Forest (RF)

Random Forest classifier provides the best accuracy with multimodal neuroimaging data, reduces overfitting problems, and can handle non-

Table 7
Comparison between different feature extraction methods for AD classification.

Feature Extraction Method	Advantages	Disadvantages
Predefined ROI Based Approaches	ROI techniques specially deal with the affected part of the AD brain like hippocampal shape, volume, size, amygdala, and ventricles thus useful for AD diagnosis at an early stage (Astrakas and Argyropoulou, 2010). This approach can provide good classification accuracy for AD/MCI or $N_{rm}C$ /MCI which is a big challenge among researchers.	For accurate ROI segmentation, it is essential to know about the magnitude and spatial pattern of AD which depends upon prior data and expert knowledge. ROI selection is a big problem. Manual segmentation of ROI and ROI selection in multiple slices is very time-consuming. Inter- and intra-observer variableness are required to be examined with statistical methods ROI techniques are hard to implement in longitudinal studies due to the difficulty of reproducing ROI from one image to the other (Astrakas and Argyropoulou, 2010).
Voxel-Based Morphometry (VBM)	VBM deals with the study of minute differences in brain anatomy by using statistical parametric mapping (SPM) and thus, it is very helpful in extracting voxel-based features (Ashburner and Friston, 2001). VBM is used for volumetric analysis, especially for grey matter in AD, and MCI patients.	VBM is not used for imperfectly registered images (Bookstein, 2001). Furthermore, motion artifacts during MRI acquisition may create problems during tissue segmentation and result in systematic classification differences (Ashburner and Friston, 2001). VBM is influenced by group differences that are localized in space (Davatzikos, 2004).
Cortical Surface-Based Methods	Cortical thickness measurement is less operator-dependent in comparison to the hippocampal volume measurements and is quite worthy for localization and quantification (Querbes et al., 2009).	Analysis of clinical data has shown the limitations of vertex-based features in the prognosis of AD i.e., in predicting whether MCI develops into AD or not (Mueller et al., 2005; Venneri, 2007; Petersen, 2003).
Wavelet transform Based	Wavelet transform nicely captures high-frequency variation in grey matter density and provides structural analysis. It provides whole-brain analysis and there is no need for segmentation (Lahmiri and Boukadoum, 2013; Davatzikos et al., 2003).	It provides a limited amount of directional sensitivity in the 3-D image (Jones et al., 2000).
Feature Extraction using Texture Analysis	AD is caused due to deposition of unwanted proteins like neurofibrillary tangles and amyloid-beta. The presence of these proteins is not captured by the current clinical MRI in the early stages of AD. However, their cumulative deposition on the brain tissues results in changing the pixel intensity of MR images which is obtained by texture analysis (TA) (Cai et al., 2020).	Texture Analysis of MR images faces challenges in its clinical use due to the lack of standardization. The acquisition of parameters, discretization of image intensities, MRTA software, and approaches all lead to MRTA heterogeneity (Cai et al., 2020).

linear data (Sarica et al., 2017). Random Forest is based on the embedded mode of classifier learning as it trains the different decision tree classifiers in parallel. In ensemble mode, more than one classifier is used, and each classifier is trained on a separate training dataset. The final classification depends on the majority of votes from the classifier (Parikh and Polikar, 2007). Lebedev et al. (2014) achieved 88.6% sensitivity and 92.0% specificity through Random Forest classifier by using a combination of both volumetric and cortical thickness features. Dimitriadis et al. (2018) used Random Forest in ensemble mode and combined multiple MRI features for simultaneously classifying all four classes AD, $N_{rm}C$, sMCI, and pMCI.

4.3. *Artificial Neural Network*

Artificial Neural Network (ANN) models are designed to process information in the same way as the human brain does (Shanmuganathan, 2016). Wang et al (Wang et al., 2019). used different classifiers and observed ANN be the best one providing an accuracy of 92.1%. The authors used urine and blood as biomarkers for evaluating AD classification performance. Deng et al (Deng et al., 1998). used ANN and obtained good classification accuracy between AD and $N_{rm}C$. Huang et al (Huang et al., 2008). used the VBM technique with single layer ANN to classify AD from $N_{rm}C$. García-Pérez et al. (1998) used artificial neural network technology to propose the differential diagnosis of AD and Vascular Dementia. Recently deep learning, which is a stratified ANN, has emerged as an excellent technique for capturing atrophies in diseased brains and thus helped in achieving improved AD classification results (Brosch et al., 2013; Liu et al., 2014b).

4.4. *Extreme Learning Machine (ELM)*

ELM is a single hidden layer feed-forward network and has shorter computational time than ANN. The reason is that ANN continuously assigns hidden nodes while ELM randomly allots hidden nodes (Huang et al., 2012). Jha et al. (2018) used an ELM classifier with DTCWT, PCA, and LDA for AD classification and obtained $90.3 \pm 1.8\%$ accuracy using the ADNI dataset and $95.7 \pm 1.5\%$ accuracy with the OASIS dataset.

4.5. ***k-Nearest Neighbor (k-NN)***

A k-NN classifies the test data based on similarity or distance measures between test and training data. A k-NN classifier selects the number of nearest neighbors (k) and calculates the distance between the test data and training data. Then it finds the neighbors having a minimum distance and assigns its class to the test data (Zhang, 2016). Vaithinathan et al. (2019) obtained textural features from different slices of 3-D MR Images and classified them using classifiers viz. RF, Linear SVM, and k-NN. The authors obtained an accuracy of 87.4%,87.4%, and 82.6%with k-NN, RF, and Linear SVM respectively in AD vs $N_{rm}C$ classification. Garg and Chaudhary (2021) evaluated the performance of nine different classifiers on mean energy features and observed k-NN as the best performer with an accuracy of 97.5% in AD/ $N_{rm}C$ classification.

4.6. ***Naive Bayes***

The Naive Bayes classifier requires very little training data, produces remarkable results, and is fast in computation as well (Friedman et al., 1997). It is suitable for multiclass problems also. Liu et al. (2013b) proposed the Multifold Bayesian Kernelization (MBK) method, which

supports different kernels for multimodal biomarkers. The aim behind this was to combine the outcome of the individual biomarker for AD vs MCI classification. Plant et al. (2010) used three different classifiers viz. SVM, Voting Feature Intervals (VFI), and Naive Bayes. The Naive Bayes classifier uses a probability density function for classification. The VFI classifies the dataset by assigning intervals for the individual feature of each class. Each feature delivers votes to the classes and the class with the maximum votes is considered the anticipated class. The authors obtained 92.0% accuracy with AD and $N_{rm}C$ classification. Bhagya Shree and Sheshadri (2018) used a Naive Bayesian Classifier for AD/ $N_{rm}C$ classification using neurocognitive tests. Kruthika et al. (2019) combined the automatic classification technique with professional radiologists' knowledge to increase the classification accuracy. The authors used a multistage classifier with Naive Bayes in the first stage for binary classification, SVM and k-NN in the second stage for binary classification and multiclass classification respectively. The Particle Swarm Optimization technique was applied for feature selection. The multistage classifier performed well for AD detection in comparison to the individual classifier such as Naive Bayes, k-NN, and SVM.

Support Vector Machine (SVM) classification produces good AD classification accuracy among other classifiers. Gupta et al. (2019a) used k-NN, RF, and SVM for classifying AD from Normal controls and achieved accuracy up to 93.1% with SVM. Rallabandi et al. (2020) extracted cortical thickness from both the right and left hemispheres of the brain and used different classifiers viz. Random Forest, Decision Tree, Naive Bayes, k-Nearest Neighbor, Linear SVM, Non-linear SVM (RBF kernel) for classification. These authors observed the best accuracy percentages at different stages of Alzheimer's through Non-linear SVM (RBF kernel). Selection criteria for various classifiers are shown in Table 8.

Table 8 shows that different classifiers perform differently with the same dataset. SVM performs well with a dataset that has a clear margin of divisions among the classes and has limited parameters so is good for the prediction of high-dimensional data. Due to its kernel nature, SVM can handle multiclass problems. SVM is more generalized and not good for overlapping targets (Nalepa and Kawulok, 2019). A k-NN is best when the dataset is labelled, and features are normalized (Zhang, 2001). Naive Bayes performs better in cases when features are independent of each other (Bielza and Larrañaga, 2014).

Table 8
Selection Criteria of different classifiers in prominent AD classification studies.

AUTHOR	Feature extraction	Database	Classifier	Performance	Selection Criteria of Classifier
Kloppel et al. (2008)	VBM	From multiple scanners and different centers	SVM (linear)	**AD / $N_{rm}C$** (ACY=95.6, SNY=97.1, SPY=94.1)	The linear kernel deals with linearly separable data. It is not suitable for non-linear data A large number of features makes the probability that the data are linearly separable (Fu et al., 2010).
Zhang et al. (2015)	PCA	OASIS	SVM (polynomial)	**AD / $N_{rm}C$** (ACY=92.4, SNY=83.5, SPY=94.9)	The polynomial kernel can deal with linearly inseparable data efficiently which linear SVM cannot do efficiently. It is suitable when a smaller number of features are present (Mejía-Guevara and Kuri-Morales, 2007).
Lebedev et al. (2014)	41 ROI	ADNI	RF	**AD / $N_{rm}C$** (SNY=88.6, SPY=92.0) **pMCI / sMCI** (SNY=81.3, SPY=83.3)	Random Forest can be used when the dataset is large, and interpretability is not a major concern. It can handle a large number of features (Breiman, 2001).
Gupta et al. (2019a)	HV+CSC+VBM	NRCD	k-NN	**AD / $N_{rm}C$** (ACY=89.4, SNY=93.8, SPY=88.3) **pMCI/ sMCI** (ACY=73.9, SNY=70.6, SPY=83.3)	The k-NN works best with normalized or scaled data. It performs well in the case of multiclass classification but must be used for small datasets. It requires labelled data. The dataset should not be noisy. A k-NN is good in the case where high accuracy is required (Zhang, 2001).
			RF	**AD / $N_{rm}C$** (ACY=88.2, SNY=78.3, SPY=92.5) **pMCI / sMCI** (ACY=78.3, SNY=76.9, SPY=80.0)	Random Forest can be used when the dataset is large, and interpretability is not a major concern. It can deal with a large number of features (Breiman, 2001).
			SVM	**AD / $N_{rm}C$** (ACY=93.1, SNY=87.9, SPY=95.6) **pMCI / sMCI** (ACY=86.9, SNY=77.8, SPY=92.8)	SVM works better with a large number of dimensions. Different Kernels of SVM can handle nonlinear data also. SVM is not good for overlapping targets (Nalepa and Kawulok, 2019).
Jha et al. (2018)	PCA+LDA	OASIS	ELM	**AD /$N_{rm}C$** (ACY=95.7 ±1.5, SNY=96.6±2.3, SPY=93.0±1.7)	ELM is suitable for small datasets. It has a short training time and better generalization capability but is not suitable for large datasets with high dimensions (Huang et al., 2012).
		ADNI		**AD / $N_{rm}C$** (ACY=90.3 ±1.2, SNY=90.3±1.3, SPY=90.2±1.6)	
Vaithinathan et al. (2019)	Fisher score+Elastic net+Recursive Feature Elimination	ADNI	k-NN	**AD / $N_{rm}C$** (ACY=87.4, SNY=89.6, SPY=85.8) **pMCI / sMCI** (ACY=66.4, SNY=60.2, SPY=69.8)	The k-NN works best with normalized or scaled data. It performs well in the case of multiclass classification but must be used for small datasets. It requires labelled data. The dataset should not be noisy. A k-NN is good in the case where high accuracy is required (Zhang, 2001).
			RF	**AD / $N_{rm}C$** (ACY=87.4, SNY=85.4, SPY=88.8) **pMCI / sMCI** (ACY=61.6, SNY=65.1, SPY=59.7)	Random Forest can be used when the dataset is large, and interpretability is not a major concern. It can deal with a large number of features (Breiman, 2001).
			Linear SVM	**AD / $N_{rm}C$** (ACY=82.6, SNY=78.1, SPY=85.8) **pMCI / sMCI** (ACY=64.7, SNY=56.6, SPY=69.1)	The linear kernel deals with linearly separable data. It is not suitable for non-linear data A large number of features makes the probability that the data are linearly separable (Fu et al., 2010).

ELM = Extreme Learning Machine Accuracy=ACY, Sensitivity=SNY, Specificity=SPY

5. Recent emerging directions for classification and prediction of Alzheimer's disease

Nowadays multimodal techniques are in trend for AD classification (Perrin et al., 2009). Multimodal techniques are beneficial as they provide features obtained from different modalities viz. Positron Emission Tomography (PET), Single-Photon Emission Computed Tomography (SPECT), MRI, Computerized Axial Tomography (CAT), etc (Liu et al., 2015b). Dukart et al. (2013) used multi modalities like MRI and fluorodeoxyglucose-PET from two datasets viz. Leipzig and ADNI datasets. The authors obtained volume-of-interest information from both MRI and fluorodeoxyglucose-PET and combined the information for SVM based AD/NC classification. The authors obtained 85.7% accuracy with the ADNI dataset and 100.0% accuracy with the Leipzig dataset. This study concluded that the approach of combining the volume of interest information from MRI and fluorodeoxyglucose-PET would give better AD/NC discrimination results in comparison to the information obtained from a single modality. Dinesh et al. (2013) used multi-modalities viz. fMRI, PET, and SPECT in their work. The authors used the Nonnegative Matrix Factorization (NMF) (Wang and Zhang, 2012), Fisher's discriminant ratio, and SVM for feature reduction, feature selection, and classification respectively, and obtained 91.0% accuracy in AD vs $N_{rm}C$ classification. Dyrba et al. (2015) used three modalities viz. Diffusion Tensor Imaging (DTI), MRI, and functional MRI. The authors obtained features such as fiber tract integrity by using DTI, GM volume through structural MRI, local clustering coefficient, and smallest path distance with the help of resting-state functional MRI (rs-fMRI). Individual and multimodal performance of all imaging modalities was evaluated by using SVM classifier. The authors obtained an accuracy of 74.0% for rs-fMRI, 85.0% for DTI, 81.0% for GM volume, and 79.0% for multimodal analysis in AD vs $N_{rm}C$ classification. This study concluded that results obtained from multimodal imagining and single modalities were not quite different.

The second most widely used technique today is the deep learning-based AD classification technique. Deep learning has the power to extract features that are hidden in the data. It can handle unstructured data and provides good results. It permits parallel processing (Venugopalan et al., 2021). The Deep Learning model is a multi-layer neural network. In deep learning, the model is trained through a large, labelled data set (Valliani et al., 2019). Helaly et al. (2021) proposed an end-to-end architecture for multi-class classification of four stages of the AD progression using Convolutional Neural Networks (CNN) and a transfer learning approach. The authors achieved an accuracy of 93.6% and 95.2% for 2-D and 3-D MR images respectively with the CNN approach and 97.0% with the transfer learning approach. In transfer learning, the training of the classifier does not start from scratch but relies on the previously learned tasks. Ramzan et al. (2019) proposed a deep residual neural network with a transfer learning approach for multi-class classification of six AD stages viz. AD, $N_{rm}C$, Significant Memory Concern (SMC), Early Mild Cognitive Impairment (EMCI), MCI, and Late Mild Cognitive Impairment (LMCI). SMC subjects show normal cognitive ability with minor memory problems. Old memories are retained with the patients, and it is difficult for them to register new memories. The Authors used rs-fMRI brain images and trained the processed images using Off-the-Shelf, 1-Channel ResNet-18, and the Fine-Tuning networks. The input image size and the pre-trained network's input size were made equal by modifying the input image size to 224×224 pixels. Initially, the model was set with a learning rate of 0.001, a Gamma value of 0.1, a momentum value of 0.9, and a weight decay factor of 0.0005. Among all models, the Off-the-Shelf based network model yielded the best performance with an accuracy of 97.9%. Liu et al. (2020) proposed a Convolutional Neural Network (CNN) based on a multi-modal deep learning model for jointly learning automatic hippocampal segmentation with AD classification. Initially, a multi-task deep CNN framework had been designed for hippocampal segmentation. Next, extracted features from the 3-D patches obtained from hippocampal segmentation were used to train 3-D Densely Connected Convolutional Networks (3-D DenseNet). Disease status was classified based on the combined results obtained through the features learned by CNN and DenseNet models.

6. Major challenges faced by AD classification studies

There have been difficulties in the classification of Alzheimer's disease from normal controls. Clinical use of classifiers faces challenges in showing generalizability to new patient data. CAD Dementia 2015 challenge (Bron et al., 2015) was proposed to compare the performance of different algorithms proposed by different researchers for AD diagnosis. This challenge is a competitive event that provides the same clinically approved dataset for implementing the algorithms and helps in addressing the clinical applicability and generalizability issues.

The classifier performance is mainly dependent on the dataset size. Smaller datasets do not sufficiently provide the heterogeneity among the different classes, therefore, lack generalization ability on new image data. The larger datasets create the problem of overfitting. Hence, an optimum size of the dataset is to be selected to train the classifier to get accurate results. Researchers are facing the problem of high dimensionality in sMCI vs pMCI classification due to the limited size of datasets (Agarwal et al., 2021).

Heterogeneity of neurodegeneration patterns in AD patients also causes difficulty in AD diagnosis (Komarova and Craig, 2011). An AD neurodegeneration pattern usually follows a pattern as described in the Braak staging (Braak and Braak, 1991) and in case it does not follow, is called atypical AD. Murray et al. (2011) compared the performance of clinical and neuropathological features for typical and atypical AD cases and observed that AD had distinct clinicopathological subtypes. Goyal et al. (2018) worked on longitudinal clinical and neuroimaging biomarkers and demonstrated heterogeneity in AD progression.

7. Conclusion and future direction

Alzheimer's disease is a severe neurological disorder that eventually leads to a person's death. This disease is spreading among elderly people at a great pace all over the world. An automated diagnostic system helps in assuring that neurologists don't need to second-guess their diagnoses and medical recommendations. These techniques help neurologists in doing the first-round classification of patients. Based on the diagnosis patients may be recommended to a neurosurgeon also. Thus, automated techniques help in the fast and precise detection of AD. Researchers are focusing on automatic AD diagnosis by using a classification approach with brain images. Feature extraction has a prominent role in AD classification. In this paper, we have included various studies based on feature extraction methods for AD classification using MR images. The strength and weaknesses of all studies along with their comparative performance are discussed in the paper. It is observed from the comparative performance that the wavelet transform-based feature extraction method is giving more promising results with an average performance of 94.5% in AD/ $N_{rm}C$ classification, followed by Cortical (92.2%), VBM (89.2%), ROI (88.1%), and Texture based technique (88.0%). The problem with the ROI technique is the accurate segmentation. VBM techniques need proper registration of images over templates. The cortical method is generally performed using Free surfer software which needs expertise. Wavelet transform methods do not need segmentation and are applied over the whole brain. The wavelet transform-based approach Alam et al. (2017) provides the best results among all discussed studies but problem is that PCA is used in this study due to which spatial information is lost. In the future, some strategies can be adopted to maintain spatial information to improve the classification results. The present review paper also reveals the comparative analysis of recent work done in AD classification using machine learning algorithms viz. Naive Bayes, SVM, ANN, k-NN, and Random Forest for AD diagnosis. SVM classifier is trending for AD classification.

It can be concluded from the literature survey that a significant level of accuracy is obtained in the domain of AD/ $N_{rm}C$ and $N_{rm}C$ /MCI classification. There are less significant results with the classification of MCI/AD and sMCI/pMCI. The future direction for research in early AD detection needs extensive studies around the classification of MCI vs AD and sMCI vs pMCI. Though there are multiple feature extraction techniques used for AD classification, still there is a need for relevant biomarkers which can reduce the redundancy, increase the classification accuracy, and can help in early AD detection. Focus is needed on enhancing the use of machine learning techniques. The feature selection process is the backbone of any classification technique. Extraction of a new set of vulnerable attributes will help in early AD detection. The literature survey indicates that there is more focus on the feature extraction and selection methods for improving the AD classification accuracy while less effort is seen in the realm of designing a novel classifier that can especially handle the neuroimaging data. Thus, efforts need to be focused on the designing phase for improving accuracy. Future research should focus on the consideration of heterogeneity of AD, using deep learning approaches and multimodal image data of patients for classification of AD vs $N_{rm}C$. Deep Learning approaches are good in handling high dimensional data and have shown outstanding performance over traditional machine learning with multimodal data.

CRediT authorship contribution statement

Neha Garg: Literature review, Writing – original draft. **Mahipal Singh Choudhry**: Supervision, Writing – review & editing. **Rajesh M Bodade**: Conceptualization, Technical editing.

Declaration of Competing Interest

The authors declare that they have no known competing financial interests or personal relationships that could have appeared to influence the work reported in this paper.

Data Availability

No data was used for the research described in the article.

References

Abdi, Hervé, Lynne, J.Williams, 2010. Principal component analysis. Wiley Interdiscip. Rev.: Comput. Stat. 2 (4), 433–459.

Abu Alfeilat, H.A., Hassanat, A.B.A., Lasassmeh, O., et al., 2019. Effects of distance measure choice on k-nearest neighbor classifier performance: a review. Big Data 7 (4), 221–248. https://doi.org/10.1089/big.2018.0175.

Acharya, U.R., Fernandes, S.L., WeiKoh, J.E., et al., 2019. Automated detection of Alzheimer's disease using brain MRI images– a study with various feature extraction techniques. J. Med Syst. 43, 302. https://doi.org/10.1007/s10916-019-1428-9.

Achterberg, Hakim C., et al., 2014. Hippocampal shape is predictive for the development of dementia in a normal, elderly population. Hum. Brain Mapp. 35 (5), 2359–2371. https://doi.org/10.1002/hbm.22333.

Agarwal, Deevyankar, et al., 2021. Transfer learning for Alzheimer's disease through neuroimaging biomarkers: a systematic review, 31 Oct Sens. (Basel, Switz.) 21 (21), 7259. https://doi.org/10.3390/s21217259, 31 Oct.

Alam, Saruar, et al., 2017. Twin SVM-based classification of Alzheimer's disease using complex dual-tree wavelet principal coefficients and LDA. J. Healthc. Eng. 2017, 8750506 https://doi.org/10.1155/2017/8750506.

Almuzian, Mohammed, et al., 15 . 2018. Assessing the validity of ITK-SNAP software package in measuring the volume of upper airway spaces secondary to rapid maxillary expansion. J. Orthod. Sci. vol. 7, 7. https://doi.org/10.4103/jos.JOS_93_17.

Alobaidli, S., et al., 2014. The role of texture analysis in imaging as an outcome predictor and potential tool in radiotherapy treatment planning. Br. J. Radiol. 87 (1042), 20140369 https://doi.org/10.1259/bjr.20140369.

Alvarez, Ignacio, et al., 2009. Alzheimer's diagnosis using eigenbrains and support vector machines. International Work-Conference on Artificial Neural Networks. Springer,, Berlin, Heidelberg.

Andrea Mechelli, Cathy J., Price, Karl J., Friston, Ashburner, John, 2005. Voxel-based morphometry of the human brain: methods and applications. Curr. Med. Imaging 1, 105. https://doi.org/10.2174/1573405054038726.

Anticevic, Alan, et al., 2008. Comparing surface-based and volume-based analyses of functional neuroimaging data in patients with schizophrenia. Neuroimage 41 (3), 835–848.

Armstrong Armstrong, E., et al., 1995. The ontogeny of human gyrification. Cereb. Cortex (N. Y., N. Y.: 1991) vol. 5 (1), 56–63. https://doi.org/10.1093/cercor/5.1.56.

Ashburner, J., et al., 1998. Identifying global anatomical differences: deformation-based morphometry. Hum. Brain Mapp. vol. 6 (5–6), 348–357 doi:10.1002/(SICI)1097-0193(1998)6:5/6<348: AID-HBM4>3.0.CO;2-P.

Ashburner, J., Friston, K.J., 2000. Voxel-based morphometry–the methods. NeuroImage vol. 11 (6 Pt 1), 805–821. https://doi.org/10.1006/nimg.2000.0582.

Ashburner, J., Friston, K.J., 2001. Why voxel-based morphometry should be used. NeuroImage vol. 14 (6), 1238–1243. https://doi.org/10.1006/nimg.2001.0961.

Ashburner, John, 2007. A fast diffeomorphic image registration algorithm. NeuroImage vol. 38 (1), 95–113. https://doi.org/10.1016/j.neuroimage.2007.07.007.

Astrakas, L.G., Argyropoulou, M.I., 2010. Shifting from region of interest (ROI) to voxel-based analysis in human brain mapping. Pedia Radio. 40, 1857–1867. https://doi.org/10.1007/s00247-010-1677-8.

Ayodele, Taiwo Oladipupo, 2010. Types of machine learning algorithms. N. Adv. Mach. Learn. 3, 19–48.

Bakkour, Akram, et al., 2009. The cortical signature of prodromal AD: regional thinning predicts mild AD dementia. Neurology vol. 72 (12), 1048–1055. https://doi.org/10.1212/01.wnl.0000340981.97664.2f.

Barburiceanu, S., Terebes, R., Meza, S., 2021. 3D texture feature extraction and classification using GLCM and LBP-based descriptors. Appl. Sci. 11, 2332.

Barnes, Josephine, et al., 2006. Measurements of the amygdala and hippocampus in pathologically confirmed Alzheimer disease and frontotemporal lobar degeneration. Arch. Neurol. vol. 63 (10), 1434–1439. https://doi.org/10.1001/archneur.63.10.1434.

Baskar, D., Jayanthi, V.S., Jayanthi, A.N., 2019. An efficient classification approach for detection of Alzheimer's disease from biomedical imaging modalities. Multimed. Tools Appl. 78 (10), 12883–12915.

Beheshti, I., et al., 2015. Probability distribution function-based classification of structural MRI for the detection of Alzheimer's disease. Comput. Biol. Med. vol. 64, 208–216. https://doi.org/10.1016/j.compbiomed.2015.07.006.

Beheshti, Iman, et al., 2017. Classification of Alzheimer's disease and prediction of mild cognitive impairment-to-Alzheimer's conversion from structural magnetic resource imaging using feature ranking and a genetic algorithm. Comput. Biol. Med. vol. 83, 109–119. https://doi.org/10.1016/j.compbiomed.2017.02.011.

Ben Ahmed, O., Benois-Pineau, J., Allard, M., et al., 2015. Classification of Alzheimer's disease subjects from MRI using hippocampal visual features. Multimed. Tools Appl. 74, 1249–1266. https://doi.org/10.1007/s11042-014-2123-y.

Bhagya Shree, S.R., Sheshadri, H.S., 2018. Diagnosis of Alzheimer's disease using Naive Bayesian Classifier. Neural Comput. Applic 29, 123–132. https://doi.org/10.1007/s00521-016-2416-3.

Bhasin, H., Agrawal, R.K., For Alzheimer's Disease Neuroimaging Initiative, 2020. A combination of 3-D discrete wavelet transforms and 3-D local binary pattern for classification of mild cognitive impairment. BMC Med Inf. Decis. Mak. 20, 37. https://doi.org/10.1186/s12911-020-1055-x.

Bielza, Concha, Larrañaga, Pedro, 2014. Bayesian networks in neuroscience: a survey, 16 Oct Front. Comput. Neurosci. vol. 8, 131. https://doi.org/10.3389/fncom.2014.00131, 16 Oct.

Bjoern Menze, Georg, Langs, Albert, Montillo, Michael, Kelm, Henning, Müller, Tu, Zhuowen, 2014. Medical Computer Vision. Large Data in Medical Imaging: Third International MICCAI Workshop, MCV 2013,Nagoya, Japan, September 26, 2013. In: Revised Selected Papers, volume 8331. Springer,.

Blennow, Kaj, 2004. Cerebrospinal fluid protein biomarkers for Alzheimer's disease. NeuroRx: J. Am. Soc. Exp. Neurother. vol. 1 (2), 213–225. https://doi.org/10.1602/neurorx.1.2.213.

Bookstein, F.L., 2001. Voxel-based morphometry" should not be used with imperfectly registered images. NeuroImage vol. 14 (6), 1454–1462. https://doi.org/10.1006/nimg.2001.0770.

Braak, H., Braak, E., 1991. Neuropathological stageing of Alzheimer-related changes. Acta Neuropathol. 82, 239–259. https://doi.org/10.1007/BF00308809.

Breiman, L., 2001. Random forests. Mach. Learn. 45, 5–32. https://doi.org/10.1023/A:1010933404324.

Bron, E.E., Smits, M., van der Flier, W.M., Vrenken, H., Barkhof, F., Scheltens, P., Papma, J.M., Steketee, R.M., Mendez Orellana, C., Meijboom, R., et al., 2015. Standardized evaluation of algorithms for computer-aided diagnosis of dementia based on structural MRI: the CADDementia challenge. Neuroimage 111, 562–579.

Brookmeyer, Ron, et al., 2007. Forecasting the global burden of Alzheimer's disease. Alzheimer's Dement. J. Alzheimer's Assoc. vol. 3 (3), 186–191. https://doi.org/10.1016/j.jalz.2007.04.381.

Brosch, Tom, et al., 2013. Manifold learning of brain MRIs by deep learning. Medical image computing and computer-assisted intervention: MICCAI. Int. Conf. Med. Image Comput. Comput. -Assist. Interv. vol. 16 (Pt 2), 633–640. https://doi.org/10.1007/978-3-642-40763-5_78.

Buchanan, R.W., et al., 1998. Structural evaluation of the prefrontal cortex in schizophrenia. Am. J. Psychiatry vol. 155 (8), 1049–1055. https://doi.org/10.1176/ajp.155.8.1049.

Cai, Jiahui, et al., 2020. Magnetic resonance texture analysis in Alzheimer's disease. Acad. Radiol. vol. 27 (12), 1774–1783. https://doi.org/10.1016/j.acra.2020.01.006.

Camara-Rey, Oscar, et al. "Simulation of local and global atrophy in Alzheimer's disease studies." International Conference on Medical Image Computing and Computer-Assisted Intervention. Springer, Berlin, Heidelberg, 2006.

Chaddad, Ahmad, et al., 2017. Hippocampus and amygdala radiomic biomarkers for the study of autism spectrum disorder. BMC Neurosci. 18 (1), 1–12.

Chandra, Avinash, et al., 2019. Magnetic resonance imaging in Alzheimer's disease and mild cognitive impairment. J. Neurol. vol. 266 (6), 1293–1302. https://doi.org/10.1007/s00415-018-9016-3.
Chen, Ying, Feng Yu Yang, 2012. Analysis of image texture features based on gray level co-occurrence matrix. In: Applied Mechanics and Materials, Vol. 204. Trans Tech Publications Ltd,.
Cho, Youngsang, et al., 2012. Individual subject classification for Alzheimer's disease based on incremental learning using a spatial frequency representation of cortical thickness data. NeuroImage vol. 59 (3), 2217–2230. https://doi.org/10.1016/j.neuroimage.2011.09.085.
Chupin, Marie, et al., 2009. Fully automatic hippocampus segmentation and classification in Alzheimer's disease and mild cognitive impairment applied on data from ADNI. Hippocampus vol. 19 (6), 579–587. https://doi.org/10.1002/hipo.20626.
Clarkson, Matthew J., et al., 2011. A comparison of voxel and surface-based cortical thickness estimation methods. NeuroImage vol. 57 (3), 856–865. https://doi.org/10.1016/j.neuroimage.2011.05.053.
Colliot, Olivier, et al., 2008. Discrimination between Alzheimer disease, mild cognitive impairment, and normal aging by using automated segmentation of the hippocampus. Radiology vol. 248 (1), 194–201. https://doi.org/10.1148/radiol.2481070876.
Cook, J.A., Ranstam, J., 2016. Overfitting. Br. J. Surg. vol. 103 (13), 1814. https://doi.org/10.1002/bjs.10244.
Coupé, Pierrick, et al., 2011. Patch-based segmentation using expert priors: application to hippocampus and ventricle segmentation. NeuroImage vol. 54 (2), 940–954. https://doi.org/10.1016/j.neuroimage.2010.09.018.
Cuingnet, R.émi, et al., 2011. Automatic classification of patients with Alzheimer's disease from structural MRI: a comparison of ten methods using the ADNI database. NeuroImage vol. 56 (2), 766–781. https://doi.org/10.1016/j.neuroimage.2010.06.013.
Dash, Sonali, Manas Ranjan Senapati, 2021. Gray level run length matrix based on various illumination normalization techniques for texture classification. Evolut. Intell. 14 (2), 217–226.
Davatzikos, C., et al., 2008a. Individual patient diagnosis of AD and FTD via high-dimensional pattern classification of MRI. NeuroImage vol. 41 (4), 1220–1227. https://doi.org/10.1016/j.neuroimage.2008.03.050.
Davatzikos, Christos, et al., 2001. Voxel-based morphometry using the RAVENS maps: methods and validation using simulated longitudinal atrophy. NeuroImage 14 (6), 1361–1369.
Davatzikos, Christos, 2004. Why voxel-based morphometric analysis should be used with great caution when characterizing group differences. NeuroImage vol. 23 (1), 17–20. https://doi.org/10.1016/j.neuroimage.2004.05.010.
Davatzikos, Christos, et al., 2008b. Detection of prodromal Alzheimer's disease via pattern classification of magnetic resonance imaging. Neurobiol. Aging vol. 29 (4), 514–523. https://doi.org/10.1016/j.neurobiolaging.2006.11.010.
Davatzikos, Christos, et al., 2011. Prediction of MCI to AD conversion, via MRI, CSF biomarkers, and pattern classification, 2322.e19-e27 Neurobiol. Aging vol. 32 (12). https://doi.org/10.1016/j.neurobiolaging.2010.05.023.
Davatzikos, Christos, Tao, Xiaodong, Shen, Dinggang, 2003. Applications of wavelets in morphometric analysis of medical images. Proc. SPIE - Int. Soc. Opt. Eng. https://doi.org/10.1117/12.504032.
De Oliveira, M.S., et al., 2011. MR imaging texture analysis of the corpus callosum and thalamus in amnestic mild cognitive impairment and mild Alzheimer disease. AJNR Am. J. Neuroradiol. vol. 32 (1), 60–66. :10.3174/ajnr. A2232.
De Siqueira, Fernando Roberti, William Robson Schwartz, Helio Pedrini, 2013. Multi-scale gray level co-occurrence matrices for texture description. Neurocomputing 120, 336–345.
Deng, X., et al., 1998. Application of artificial neural network in the MRI study of Alzheimer disease. Chin. J. Radiol. 812–816.
Desai, Rutvik, et al., 2005. Volumetric vs. surface-based alignment for localization of auditory cortex activation. Neuroimage 26 (4), 1019–1029.
De-Shuang Huang, Donald C. Wunsch, Daniel S. Levine, and Kang-Hyun Jo. Advanced Intelligent Computing Theories and Applications. With Aspects of Theoretical and Methodological Issues: Fourth International Conference on Intelligent Computing, ICIC 2008 Shanghai, China, September 15–18, 2008 Proceedings, volume 5226. Springer, 2008.
Desikan, Rahul S., et al., 2006. An automated labeling system for subdividing the human cerebral cortex on MRI scans into gyral based regions of interest. NeuroImage vol. 31 (3), 968–980. https://doi.org/10.1016/j.neuroimage.2006.01.021.
Desikan, Rahul S., et al., 2009. Automated MRI measures identify individuals with mild cognitive impairment and Alzheimer's disease. Brain: a J. Neurol. vol. 132 (Pt 8), 2048–2057. https://doi.org/10.1093/brain/awp123.
Dickerson, Bradford C., et al., 2009a. The cortical signature of Alzheimer's disease: regionally specific cortical thinning relates to symptom severity in very mild to mild AD dementia and is detectable in asymptomatic amyloid-positive individuals. Cereb. Cortex (N. Y., N. Y.: 1991) vol. 19 (3), 497–510. https://doi.org/10.1093/cercor/bhn113.
Dickerson, Bradford C., et al., 2009b. Differential effects of aging and Alzheimer's disease on medial temporal lobe cortical thickness and surface area. Neurobiol. Aging vol. 30 (3), 432–440. https://doi.org/10.1016/j.neurobiolaging.2007.07.022.
Dimitriadis, S.I., et al., 2018. Random Forest feature selection, fusion and ensemble strategy: Combining multiple morphological MRI measures to discriminate among healhy elderly, MCI, cMCI and alzheimer's disease patients: From the alzheimer's disease neuroimaging initiative (ADNI) database. J. Neurosci. Methods vol. 302, 14–23. https://doi.org/10.1016/j.jneumeth.2017.12.010.
Dinesh, E., et al., 2013. Instinctive classification of Alzheimer's disease using FMRI, pet and SPECT images. 2013 7th Int. Conf. Intell. Syst. Control (ISCO) 405–409.
Doan, Nhat Trung, Jonathan Orban de Xivry, and Benoît Macq. "Effect of inter-subject variation on the accuracy of atlas-based segmentation applied to human brain structures." Medical Imaging 2010: Image Processing. Vol. 7623. International Society for Optics and Photonics, 2010.
Du, An-Tao, et al., 2007. Different regional patterns of cortical thinning in Alzheimer's disease and frontotemporal dementia. Brain J. Neurol. vol. 130 (Pt 4), 1159–1166. https://doi.org/10.1093/brain/awm016.
Dukart, Juergen, et al., 2013. Meta-analysis based SVM classification enables accurate detection of Alzheimer's disease across different clinical centers using FDG-PET and MRI. Psychiatry Res. vol. 212 (3), 230–236. https://doi.org/10.1016/j.pscychresns.2012.04.007.
Dyrba, Martin, et al., 2015. Multimodal analysis of functional and structural disconnection in Alzheimer's disease using multiple kernel SVM. Hum. Brain Mapp. vol. 36 (6), 2118–2131. https://doi.org/10.1002/hbm.22759.
El-Dahshan, E.-S.A., Hosny, T., Salem, A.-B.M., 2010. Hybrid intelligent techniques for MRI brain images classification. 'Digital Signal Process. 20 (2), 433–441.
Elsayed, A., et al. Region of Interest Based Image Classification: A Study in MRI Brain Scan Categorization. Data Mining Applications in Engineering and Medicine. 2012.
Eskildsen, Simon F., et al., 2013. Prediction of Alzheimer's disease in subjects with mild cognitive impairment from the ADNI cohort using patterns of cortical thinning. Neuroimage vol. 65, 511–521. https://doi.org/10.1016/j.neuroimage.2012.09.058.
Fan Y., Resnick S.M., Davatzikos C.Feature selection and classification of multi-parametric medical images using bagging and SVM." (2008a) Progress in Biomedical Optics and Imaging - Proceedings of SPIE, 6914, art. no. 69140Q.
Fan, Yong, et al., 2005. Classification of structural images via high-dimensional image warping, robust feature extraction, and SVM. Medical image computing and computer-assisted intervention: MICCAI. Int. Conf. Med. Image Comput. Comput. -Assist. Interv. vol. 8 (Pt 1), 1–8. https://doi.org/10.1007/11566465_1.
Fan, Yong, et al., 2007a. COMPARE: classification of morphological patterns using adaptive regional elements. IEEE Trans. Med. Imaging vol. 26 (1), 93–105. https://doi.org/10.1109/TMI.2006.886812.
Fan, Yong, et al., 2007b. Multivariate examination of brain abnormality using both structural and functional MRI. NeuroImage vol. 36 (4), 1189–1199. https://doi.org/10.1016/j.neuroimage.2007.04.009.
Fan, Yong, et al., 2008a. Spatial patterns of brain atrophy in MCI patients, identified via high-dimensional pattern classification, predict subsequent cognitive decline. NeuroImage vol. 39 (4), 1731–1743. https://doi.org/10.1016/j.neuroimage.2007.10.031.
Fan, Yong, et al., 2008b. Unaffected family members and schizophrenia patients share brain structure patterns: a high-dimensional pattern classification study. Biol. Psychiatry vol. 63 (1), 118–124. https://doi.org/10.1016/j.biopsych.2007.03.015.
Fan, Yong, et al., 2008b. Structural and functional biomarkers of prodromal Alzheimer's disease: a high-dimensional pattern classification study. NeuroImage vol. 41 (2), 277–285. https://doi.org/10.1016/j.neuroimage.2008.02.043.
Farhan, Saima, et al., 2014. An ensemble-of-classifiers based approach for early diagnosis of Alzheimer's disease: classification using structural features of brain images. Comput. Math. Methods Med. vol. 2014, 862307 https://doi.org/10.1155/2014/862307.
Feng, Feng, et al., . 2018. Radiomic features of hippocampal subregions in Alzheimer's disease and amnestic mild cognitive impairment. Front. Aging Neurosci. vol. 10 (290), 25. https://doi.org/10.3389/fnagi.2018.00290.
Fischl, B., et al., 1999. High-resolution intersubject averaging and a coordinate system for the cortical surface. Hum. brain Mapp. vol. 8 (4), 272–284. https://doi.org/10.1002/(sici)1097-0193(1999)8:4<272:aid-hbm10>3.0.co;2-4.
Fischl, B., Dale, A.M., 2000. Measuring the thickness of the human cerebral cortex from magnetic resonance images. Proc. Natl. Acad. Sci. USA vol. 97 (20), 11050–11055. https://doi.org/10.1073/pnas.200033797.
Fischl, Bruce, et al., 2002. Whole brain segmentation: automated labeling of neuroanatomical structures in the human brain. Neuron vol. 33 (3), 341–355. https://doi.org/10.1016/s0896-6273(02)00569-x.
Frey, Brendan J., Delbert, Dueck, 2007. Clustering by passing messages between data points. Science vol. 315 (5814), 972–976. https://doi.org/10.1126/science.1136800.
Friedman, N., Geiger, D., Goldszmidt, M., 1997. Bayesian network classifiers. Mach. Learn. 29, 131–163. https://doi.org/10.1023/A:1007465528199.
Frisoni, Giovanni B., et al., 2010. The clinical use of structural MRI in Alzheimer disease. Nat. Rev. Neurol. vol. 6 (2), 67–77. https://doi.org/10.1038/nrneurol.2009.215.
Fu, Zhouyu, et al., 2010. Mixing linear SVMs for nonlinear classification. IEEE Trans. Neural Netw. vol. 21 (12), 1963–1975. https://doi.org/10.1109/TNN.2010.2080319.
Gao, Ni, et al., 2018. Contourlet-based hippocampal magnetic resonance imaging texture features for multivariant classification and prediction of Alzheimer's disease. Metab. Brain Dis. vol. 33 (6), 1899–1909. https://doi.org/10.1007/s11011-018-0296-1.
Gao, Yi, and Allen Tannenbaum. Combining atlas and active contour for automatic 3D medical image segmentation. 2011 IEEE International Symposium on Biomedical Imaging: From Nano to Macro. IEEE, 2011.
García-Peŕez E, Violante A, Cervantes-Peŕez F, 1998. Using neural networks for differential diagnosis of Alzheimer disease and vascular dementia. Expert Syst. Appl. 14 (1–2), 219–225. https://doi.org/10.1016/S0957-4174(97)00076-6.
Garg, N., Chaudhary, M., 2021. Implementation of dual tree complex wavelet transform with mean energy features to detect Alzheimer's disease. 2021 7th Int. Conf. Signal Process. Commun. (ICSC) 188–193. https://doi.org/10.1109/ICSC53193.2021.9673484.

Gerardin, Emilie, et al., 2009. Multidimensional classification of hippocampal shape features discriminates Alzheimer's disease and mild cognitive impairment from normal aging. NeuroImage vol. 47 (4), 1476–1486. https://doi.org/10.1016/j.neuroimage.2009.05.036.
Ghahramani, Zoubin. Unsupervised learning. Summer school on machine learning. Springer, Berlin, Heidelberg, 2003.
Ghosh, et al., 2010. Evaluating the validity of volume-based and surface-based brain image registration for developmental cognitive neuroscience studies in children 4 to 11 years of age (Ghosh, Satrajit S et al). NeuroImage vol. 53 (1 (2010)), 85–93. https://doi.org/10.1016/j.neuroimage.2010.05.075.
Glodzik-Sobanska, Lidia, et al., 2005. The role of quantitative structural imaging in the early diagnosis of Alzheimer's disease (x). Neuroimaging Clin. North Am. vol. 15 (4), 803–826. https://doi.org/10.1016/j.nic.2005.09.004.
Goyal, Devendra, et al., 2018. Characterizing heterogeneity in the progression of Alzheimer's disease using longitudinal clinical and neuroimaging biomarkers, 10 Aug Alzheimer'S. Dement. (Amst., Neth.) vol. 10, 629–637. https://doi.org/10.1016/j.dadm.2018.06.0, 10 Aug.
Gupta, Yubraj, et al., 2019a. Early diagnosis of Alzheimer's disease using combined features from voxel-based morphometry and cortical, subcortical, and hippocampus regions of MRI T1 brain images, 4 Oct PloS One vol. 14 (10), e0222446. https://doi.org/10.1371/journal.pone.0222446.
Gupta, Yubraj, et al., 2019b. Alzheimer's disease diagnosis based on cortical and subcortical features, 3 Mar J. Healthc. Eng. vol. 2019 (2492719). https://doi.org/10.1155/2019/2492719, 3 Mar.
Hampel, H., Frank, R., Broich, K., et al., 2010. Biomarkers for Alzheimer's disease: academic, industry and regulatory perspectives. Nat. Rev. Drug Disco 9, 560–574. https://doi.org/10.1038/nrd3115.
Han, Fang, and Han Liu. Principal component analysis on non-Gaussian dependent data. International Conference on Machine Learning. PMLR, 2013.
Haralick, Robert M., Shanmugam, Karthikeyan, Dinstein, Its' Hak, 1973. Textural features for image classification. IEEE Trans. Syst., Man, Cybern. 6, 610–621.
Hawkins, Douglas M., 2004. The problem of overfitting. J. Chem. Inf. Comput. Sci. vol. 44 (1), 1–12. https://doi.org/10.1021/ci0342472.
Helaly, Hadeer A., et al., 2021. Deep learning approach for early detection of Alzheimer's disease, 3 Nov Cogn. Comput. 1–17. https://doi.org/10.1007/s12559-021-09946-2, 3 Nov.
Hua, Jianping, et al., 2005. Optimal number of features as a function of sample size for various classification rules. Bioinforma. (Oxf., Engl.) vol. 21 (8), 1509–1515. https://doi.org/10.1093/bioinformatics/bti171.
Huang, B., Yan, H., Jiang, Wang, D., 2008. Combining voxel-based morphometry with artifical neural network theory in the application research of diagnosing Alzheimer's disease. 2008 Int. Conf. Biomed. Eng. Inform., Sanya 250–254. https://doi.org/10.1109/BMEI.2008.245.
Huang, Guang-Bin, et al., 2012. Extreme learning machine for regression and multiclass classification. IEEE Trans. Syst., Man, Cybern. Part B, Cybern.: a Publ. IEEE Syst., Man, Cybern. Soc. vol. 42 (2), 513–529. https://doi.org/10.1109/TSMCB.2011.2168604.
Hutton, Chloe, et al., 2008. Voxel-based cortical thickness measurements in MRI. NeuroImage vol. 40 (4), 1701–1710. https://doi.org/10.1016/j.neuroimage.2008.01.027.
Im, et al., 2008. Sulcal morphology changes and their relationship with cortical thickness and gyral white matter volume in mild cognitive impairment and Alzheimer's disease (Im, Kiho et al). NeuroImage vol. 43 (1), 103–113. https://doi.org/10.1016/j.neuroimage.2008.07.016.
Jack Jr, Clifford R., et al., 2010. Hypothetical model of dynamic biomarkers of the Alzheimer's pathological cascade. " *Lancet Neurol.* vol. 9 (1), 119–128. https://doi.org/10.1016/S1474-4422(09)70299-6.
Jack Jr, Clifford R., et al., 2011. Steps to standardization and validation of hippocampal volumetry as a biomarker in clinical trials and diagnostic criterion for Alzheimer's disease. e4 Alzheimer'S. Dement.: J. Alzheimer'S. Assoc. vol. 7 (4), 474–485. https://doi.org/10.1016/j.jalz.2011.04.007.
Jagust, W.J., et al., 2009. Relationships between biomarkers in aging and dementia. Neurology vol. 73 (15), 1193–1199. https://doi.org/10.1212/WNL.0b013e3181bc010c.
Jaroudi, Wafa, et al., 2017. Factors underlying cognitive decline in old age and Alzheimer's disease: the role of the hippocampus. Rev. Neurosci. vol. 28 (7), 705–714. https://doi.org/10.1515/revneuro-2016-0086.
Jha, D., Kwon, G.-R., 2018. Contourlet-based feature extraction for computer-aided classification of Alzheimer's disease. Alzheimer's and Dementia, 14 (7), 1473. https://doi.org/10.1016/j.jalz.2018.06.2498.
Jha, Debesh, et al., 2018. Alzheimer's disease detection using extreme learning machine, complex dual tree wavelet principal coefficients and linear discriminant analysis. J. Med. Imaging Health Inform. 8, 881–890.
Jha, J.-I., Kim, Kwon, G.-R., 2017. Diagnosis of Alzheimer's disease using dual-tree complex wavelet transform, pca, and feed-forward neural network. J. Healthc. Eng. vol. 2017 https://doi.org/10.1155/2017/9060124.
Jia, W., Sun, M., Lian, J., et al., 2022. Feature dimensionality reduction: a review. Complex Intell. Syst. https://doi.org/10.1007/s40747-021-00637-x.
Jones, S.E., et al., 2000. Three-dimensional mapping of cortical thickness using Laplace's equation. Hum. Brain Mapp. vol. 11 (1), 12–32, 10.1002/1097-0193(200009)11:1<12: aid-hbm20>3.0.co;2-k.
Juottonen, K., et al., 1998. Major decrease in the volume of the entorhinal cortex in patients with Alzheimer's disease carrying the apolipoprotein E epsilon4 allele. J. Neurol., Neurosurg., Psychiatry vol. 65 (3), 322–327. https://doi.org/10.1136/jnnp.65.3.322.
Kalinic, Hrvoje, 2009. Atlas-based image segmentation: a survey. Croat. Sci. Bibliogr. 1–7.
Kamathe, R.S., et al., 2018. A novel method based on independent component analysis for brain MR image tissue classification into CSF, WM and GM for atrophy detection in Alzheimer's disease. Biomed. Signal Process. Control Vol.40, 41–48. https://doi.org/10.1016/j.bspc.2017.09.005.
Karas, G.B., Burton, E.J., Rombouts, S.A., et al., 2003. A comprehensive study of gray matter loss in patients with Alzheimer's disease using optimized voxel-based morphometry. Neuroimage 18 (4), 895–907. https://doi.org/10.1016/s1053-8119(03)00041-7.
Khan, Ali R., et al., 2008. FreeSurfer-initiated fully-automated subcortical brain segmentation in MRI using Large Deformation Diffeomorphic Metric Mapping. NeuroImage vol. 41 (3), 735–746. https://doi.org/10.1016/j.neuroimage.2008.03.024.
Khan, Ali R., et al., 2015. Unified voxel- and tensor-based morphometry (UVTBM) using registration confidence. Neurobiol. Aging vol. 36 (Suppl 1,Suppl 1), S60–S68. https://doi.org/10.1016/j.neurobiolaging.2014.04.036.
Khedher, Laila, et al., 2017. Independent component analysis-support vector machine-based computer-aided diagnosis system for Alzheimer's with visual support. Int. J. Neural Syst. vol. 27 (3), 1650050. https://doi.org/10.1142/S0129065716500507.
Khlif, Mohamed Salah, et al., 2019. A comparison of automated segmentation and manual tracing in estimating hippocampal volume in ischemic stroke and healthy control participants. NeuroImage. Clin. vol. 21, 101581 https://doi.org/10.1016/j.nicl.2018.10.019.
Khoury, Rita, Ghossoub, Elias, 2019. Diagnostic biomarkers of Alzheimer's disease: a state-of-the-art review. Biomark. Neuropsychiatry 1 (2019), 100005. https://doi.org/10.1016/j.bionps.2019.100005.
Killiany, R.J., et al., 2002. MRI measures of entorhinal cortex vs hippocampus in preclinical AD. Neurology vol. 58 (8), 1188–1196. https://doi.org/10.1212/wnl.58.8.1188.
Killiany, Ronald J., et al., 2000. Use of structural magnetic resonance imaging to predict who will get Alzheimer's disease. Ann. Neurol.: Off. J. Am. Neurol. Assoc. Child Neurol. Soc. 47 (4), 430–439.
Kingsbury, N., 2001. Complex wavelets for shift invariant analysis and filtering of signals. Appl. Comput. Harmon. Anal. vol. 10 (3), 234–353.
Klöppel, Stefan, et al., 2008. Automatic classification of MR scans in Alzheimer's disease. Brain 131 (3), 681–689.
Koikkalainen, Juha, et al., 2011. Multi-template tensor-based morphometry: application to analysis of Alzheimer's disease. Neuroimage vol. 56 (3), 1134–1144. https://doi.org/10.1016/j.neuroimage.2011.03.029.
Komarova, Natalia L., Craig, J.Thalhauser, 2011. High degree of heterogeneity in Alzheimer's disease progression patterns. PLoS Comput. Biol. vol. 7 (11), e1002251 https://doi.org/10.1371/journal.pcbi.1002251.
Kovalev, V.A., Kruggel, F., Gertz, H.J., et al., 2001. Three-dimensional texture analysis of MRI brain datasets. IEEE Trans. Med Imaging 20, 424–433.
Kriegeskorte, Nikolaus, et al., 2009. Circular analysis in systems neuroscience: the dangers of double dipping. Nat. Neurosci. vol. 12 (5), 535–540. https://doi.org/10.1038/nn.2303.
Kruthika, K.R., et al., 2019. Multistage classifier-based approach for Alzheimer's disease prediction and retrieval. Inform. Med. Unlocked 14, 34–42. https://doi.org/10.1016/j.imu.2018.12.003.
Kukull, W.A., et al., 1994. The Mini-Mental State Examination score and the clinical diagnosis of dementia. J. Clin. Epidemiol. vol. 47 (9), 1061–1067. https://doi.org/10.1016/0895-4356(94)90122-8.
Lahmiri, Salim, Boukadoum, Mounir, 2013. Hybrid discrete wavelet transform and gabor filter banks processing for features extraction from biomedical images. J. Med. Eng. vol. 2013, 104684 https://doi.org/10.1155/2013/104684.
Lahmiri, Salim, Boukadoum, Mounir, 2014. New approach for automatic classification of Alzheimer's disease, mild cognitive impairment and healthy brain magnetic resonance images, 16 Jun Healthc. Technol. Lett. vol. 1 (1), 32–36. https://doi.org/10.1049/htl.2013.0022, 16 Jun.
Lama, Ramesh Kumar, et al., 2017. Diagnosis of Alzheimer's disease based on structural mri images using a regularized extreme learning machine and PCA features. J. Healthc. Eng. vol. 2017, 5485080. https://doi.org/10.1155/2017/5485080.
Lao, Zhiqiang, et al., 2004. Morphological classification of brains via high-dimensional shape transformations and machine learning methods. NeuroImage vol. 21 (1), 46–57. https://doi.org/10.1016/j.neuroimage.2003.09.027.
Larry, S.Davis, 1975. A survey of edge detection techniques. Comput. Graph. Image Process. 4 (3), 248–270.
Lebedev, A.V., Westman, E., Van Westen, G.J., et al., 2014. Random Forest ensembles for detection and prediction of Alzheimer's disease with a good between-cohort robustness. PublishedAug 28 Neuroimage Clin. 2014 6, 115–125. https://doi.org/10.1016/j.nicl.2014.08.023. PublishedAug 28.
Lella, Eufemia, et al., 2021. An ensemble learning approach based on diffusion tensor imaging measures for Alzheimer's disease classification. Electronics 10, 249.
Lepore, N. et al. Multi-atlas tensor-based morphometry and its application to a genetic study of 92 twins. (2008).
Li, Gang, et al., 2009. Grouping of brain MR images via affinity propagation. . Midwest Symp. . Circuits Syst. Conf. Proc.: MWSCAS Midwest Symp. . Circuits Syst. vol. 2009, 2425–2428. https://doi.org/10.1109/ISCAS.2009.5118290.
Li, Shuyu, et al., 2014. Abnormal changes of multidimensional surface features using multivariate pattern classification in amnestic mild cognitive impairment patients. J. Neurosci.: Off. J. Soc. Neurosci. vol. 34 (32), 10541–10553. https://doi.org/10.1523/JNEUROSCI.4356-13.2014.
Libero, Lauren E., et al., 2014. Surface-based morphometry of the cortical architecture of autism spectrum disorders: volume, thickness, area, and gyrification.

Neuropsychologia vol. 62, 1–10. https://doi.org/10.1016/j.neuropsychologia.2014.07.001.
Lin, Nan, et al., 2015. Functional principal component analysis and randomized sparse clustering algorithm for medical image analysis, 21 Jul PloS One vol. 10 (7), e0132945. https://doi.org/10.1371/journal.pone.0132945, 21 Jul.
Liu, et al., 2013a. Longitudinal changes in sulcal morphology associated with late-life aging and MCI (Liu, Tao et al.). NeuroImage vol. 74 (2013), 337–342. https://doi.org/10.1016/j.neuroimage.2013.02.047.
Liu, Fayao, et al., 2014a. Multiple kernel learning in the primal for multimodal Alzheimer's disease classification. IEEE J. Biomed. Health Inform. vol. 18 (3), 984–990. https://doi.org/10.1109/JBHI.2013.2285378.
Liu, J., Li, M., Lan, W., Wu, F., Pan, Y., Wang, J., 2018. Classification of Alzheimer's disease using whole brain hierarchical network, 1 March-April " IEEE/ACM Trans. Comput. Biol. Bioinforma. vol. 15 (2), 624–632. https://doi.org/10.1109/TCBB.2016.2635144.
Liu, Manhua, et al., 2012. Ensemble sparse classification of Alzheimer's disease. NeuroImage vol. 60 (2), 1106–1116. https://doi.org/10.1016/j.neuroimage.2012.01.055.
Liu, Manhua, et al., 2014a. Hierarchical fusion of features and classifier decisions for Alzheimer's disease diagnosis. Hum. Brain Mapp. vol. 35 (4), 1305–1319. https://doi.org/10.1002/hbm.22254.
Liu, Manhua, et al., 2020. A multi-model deep convolutional neural network for automatic hippocampus segmentation and classification in Alzheimer's disease. NeuroImage vol. 208, 116459. https://doi.org/10.1016/j.neuroimage.2019.116459.
Liu, Mingxia, et al., 2015a. View-centralized multi-atlas classification for Alzheimer's disease diagnosis. Hum. Brain Mapp. vol. 36 (5), 1847–1865. https://doi.org/10.1002/hbm.22741.
Liu, Mingxia, et al., 2016a. Relationship induced multi-template learning for diagnosis of Alzheimer's disease and mild cognitive impairment. IEEE Trans. Med. Imaging vol. 35 (6), 1463–1474. https://doi.org/10.1109/TMI.2016.2515021.
Liu, Mingxia, et al., 2016b. Inherent structure-based multiview learning with multitemplate feature representation for Alzheimer's disease diagnosis, 1473-82 IEEE Trans. bio-Med. Eng. 63 (7). https://doi.org/10.1109/TBME.2015.2496233.
Liu, S., Liu, S., Cai, W., Pujol, S., Kikinis, R., Feng, D., 2014b. Early diagnosis of Alzheimer's disease with deep learning. 2014 IEEE 11th Int. Symp. . Biomed. Imaging (ISBI), Beijing 1015–1018. https://doi.org/10.1109/ISBI.2014.6868045.
Liu, Sidong, et al., 2013b. Multifold Bayesian kernelization in Alzheimer's diagnosis. Medical image computing and computer-assisted intervention: MICCAI. Int. Conf. Med. Image Comput. Comput. -Assist. Interv. vol. 16 (Pt 2), 303–310. https://doi.org/10.1007/978-3-642-40763-5_38.
Liu, Siqi, et al., 2015b. Multimodal neuroimaging feature learning for multiclass diagnosis of Alzheimer's disease. IEEE Trans. bio-Med. Eng. vol. 62 (4), 1132–1140. https://doi.org/10.1109/TBME.2014.2372011.
Long, et al., 2013. Distinct laterality alterations distinguish mild cognitive impairment and Alzheimer's disease from healthy aging: statistical parametric mapping with high-resolution MRI (Long, Xiaojing et al.). Hum. brain Mapp. vol. 34 (12), 3400–3410. https://doi.org/10.1002/hbm.22157.
Luk, Collin C., et al., 2018. Alzheimer's disease: 3-Dimensional MRI texture for prediction of conversion from mild cognitive impairment, 2 Nov Alzheimer'S. Dement. (Amst., Neth.) vol. 10, 755–763. https://doi.org/10.1016/j.dadm.2018.09.002, 2 Nov.
MacDonald, D., et al., 2000. Automated 3-D extraction of inner and outer surfaces of cerebral cortex from MRI. NeuroImage vol. 12 (3), 340–356. https://doi.org/10.1006/nimg.1999.0534.
Magnin, Benoît, et al., 2009. Support vector machine-based classification of Alzheimer's disease from whole-brain anatomical MRI. Neuroradiology vol. 51 (2), 73–83. https://doi.org/10.1007/s00234-008-0463-x.
McCarthy, Ian, et al., 24 . 2019. Detection and localization of hesitant steps in people with Alzheimer's disease navigating routes of varying complexity. Healthc. Technol. Lett. vol. 6 (2), 42–47. https://doi.org/10.1049/htl.2018.5034.
Mejía-Guevara, I., Kuri-Morales, Á., 2007. MP-Polynomial Kernel for Training Support Vector Machines. In: Rueda, L., Mery, D., Kittler, J. (Eds.), Progress in Pattern Recognition, Image Analysis and Applications. CIARP 2007. Lecture Notes in Computer Science, vol 4756. Springer, Berlin, Heidelberg. https://doi.org/10.1007/978-3-540-76725-1_61.
Min, Rui, et al., 2014. Multi-atlas based representations for Alzheimer's disease diagnosis. Hum. brain Mapp. vol. 35 (10), 5052–5070. https://doi.org/10.1002/hbm.22531.
Misra, Chandan, et al., 2009. Baseline and longitudinal patterns of brain atrophy in MCI patients, and their use in prediction of short-term conversion to AD: results from ADNI. NeuroImage vol. 44 (4), 1415–1422. https://doi.org/10.1016/j.neuroimage.2008.10.031.
Möller, Christiane, et al., 2016. Alzheimer disease and behavioral variant frontotemporal dementia: automatic classification based on cortical atrophy for single-subject diagnosis. Radiology vol. 279 (3), 838–848. https://doi.org/10.1148/radiol.2015150220.
Moon, Seok Woo, et al., 2018. Changes in the hippocampal volume and shape in early-onset mild cognitive impairment. Psychiatry Investig. vol. 15 (5), 531–537. https://doi.org/10.30773/pi.2018.02.12.
Morris, J.C., 1993. The Clinical Dementia Rating (CDR): current version and scoring rules. Neurology vol. 43 (11), 2412–2414. https://doi.org/10.1212/wnl.43.11.2412-a.
Moulin, Pierre, 2009. Multiscale image decompositions and wavelets. The Essential Guide to Image Processing. Academic Press,, pp. 123–142.
Mueller, Susanne G., et al., 2005. Ways toward an early diagnosis in Alzheimer's disease: the Alzheimer's Disease Neuroimaging Initiative (ADNI). Alzheimer'S. Dement.: J. Alzheimer'S. Assoc. vol. 1 (1), 55–66. https://doi.org/10.1016/j.jalz.2005.06.003.
Murray, Melissa E., et al., 2011. Neuropathologically defined subtypes of Alzheimer's disease with distinct clinical characteristics: a retrospective study. Lancet Neurol. vol. 10 (9), 785–796. https://doi.org/10.1016/S1474-4422(11)70156-9.
Nalepa, J., Kawulok, M., 2019. Selecting training sets for support vector machines: a review. Artif. Intell. Rev. 52, 857–900. https://doi.org/10.1007/s10462-017-9611-1.
Nestor, Sean M., et al., 2008. Ventricular enlargement as a possible measure of Alzheimer's disease progression validated using the Alzheimer's disease neuroimaging initiative database. Brain: a J. Neurol. vol. 131 (Pt 9), 2443–2454. https://doi.org/10.1093/brain/awn146.
Ng, E.Y.K., Jamil, M., 2014. Parametric sensitivity analysis of radiofrequency ablation with efficient experimental design. Int. J. Thermal. Sci 80, 41–47.
Ng, H.P., et al. Medical image segmentation using k-means clustering and improved watershed algorithm. 2006 IEEE southwest symposium on image analysis and interpretation. IEEE, 2006.
Nor Aishah Ahad, Sharipah Soaad Syed Yahaya, 2014. Sensitivity analysis of welch'st-test. In: In AIP Conference Proceedings, volume 1605. American Institute of Physics, pp. 888–893.
Odusami, Modupe, et al., 2021. Analysis of features of Alzheimer's disease: detection of early stage from functional brain changes in magnetic resonance images using a finetuned ResNet18 network, 10 Jun Diagn. (Basel, Switz.) vol. 11 (6), 1071. https://doi.org/10.3390/diagnostics11061071, 10 Jun.
Ojala, Timo, Pietikäinen, Matti, Harwood, David, 1996. A comparative study of texture measures with classification based on featured distributions. Pattern Recognit. 29 (1), 51–59.
Ojala, Timo, Pietikainen, Matti, Maenpaa, Topi, 2002. Multiresolution gray-scale and rotation invariant texture classification with local binary patterns. IEEE Trans. Pattern Anal. Mach. Intell. 24. 7 971–987.
Oliveira Jr, Pedro Paulo de Magalhães, et al., 2010. Use of SVM methods with surface-based cortical and volumetric subcortical measurements to detect Alzheimer's disease. J. Alzheimer's Dis. JAD vol. 19 (4), 1263–1272. https://doi.org/10.3233/JAD-2010-1322.
Pang, Shumao, et al., 3 . 2017. Hippocampus segmentation based on local linear mapping. Sci. Rep. vol. 7, 45501. https://doi.org/10.1038/srep45501.
Parikh, Polikar, R., 2007. An ensemble-based incremental learning approach to data fusion (April). IEEE Trans. Syst., Man, Cybern., Part B (Cybern.) vol. 37 (2), 437–450. https://doi.org/10.1109/TSMCB.2006.883873.
Park, Hyunjin, et al., 2012. Dimensionality reduced cortical features and their use in the classification of Alzheimer's disease and mild cognitive impairment. Neurosci. Lett. vol. 529 (2), 123–127. https://doi.org/10.1016/j.neulet.2012.09.011.
Park, Hyunjin, et al., 2013. Dimensionality reduced cortical features and their use in predicting longitudinal changes in Alzheimer's disease. Neurosci. Lett. vol. 550, 17–22. https://doi.org/10.1016/j.neulet.2013.06.042.
Parvin, Hamid et al. "MKNN: Modified K-Nearest Neighbor." (2008).
Perrin, Richard, J., et al., 2009. Multimodal techniques for diagnosis and prognosis of Alzheimer's disease. Nature vol. 461 (7266), 916–922. https://doi.org/10.1038/nature08538.
Petersen, Ronald C., 2003. Mild cognitive impairment clinical trials. Nat. Rev. Drug Discov. vol. 2 (8), 646–653. https://doi.org/10.1038/nrd1155.
Pham, Tuan Anh. "Optimization of texture feature extraction algorithm." (2010).
Pirouz, Dante M. "An overview of partial least squares." Available at SSRN 1631359 (2006).
Plant, Claudia, et al., 2010. Automated detection of brain atrophy patterns based on MRI for the prediction of Alzheimer's disease. Neuroimage vol. 50 (1), 162–174. https://doi.org/10.1016/j.neuroimage.2009.11.046.
Poulin, Stéphane P., et al., 2011. Amygdala atrophy is prominent in early Alzheimer's disease and relates to symptom severity. Psychiatry Res. vol. 194 (1), 7–13. https://doi.org/10.1016/j.pscychresns.2011.06.014.
Qiu, Anqi, et al., 2008. Parallel transport in diffeomorphisms distinguishes the time-dependent pattern of hippocampal surface deformation due to healthy aging and the dementia of the Alzheimer's type. NeuroImage vol. 40 (1), 68–76. https://doi.org/10.1016/j.neuroimage.2007.11.041.
Querbes, Olivier, et al., 2009. Early diagnosis of Alzheimer's disease using cortical thickness: impact of cognitive reserve. Brain: a J. Neurol. vol. 132 (Pt 8), 2036–2047. https://doi.org/10.1093/brain/awp105.
Rallabandi, V.P.Subramanyam, Tulpule, Ketki, Gattu, Mahanandeeshwar, 2020. Automatic classification of cognitively normal, mild cognitive impairment and Alzheimer's disease using structural MRI analysis. In: Informatics in Medicine, vol 18. Elsevier. https://doi.org/10.1016/j.imu.2020.100305.
Ramzan, Farheen, et al., 2019. A deep learning approach for automated diagnosis and multi-class classification of Alzheimer's disease stages using resting-state fMRI and residual neural networks, 18 Dec J. Med. Syst. vol. 44 (2), 37. https://doi.org/10.1007/s10916-019-1475-2, 18 Dec.
Rana, Bharti, et al., 2015. Regions-of-interest based automated diagnosis of Parkinson's disease using T1-weighted MRI. Expert Syst. Appl. 42 (9), 4506–4516.

Razavi, F., Tarokh, M.J., Alborzi, M., 2019. An intelligent Alzheimer's disease diagnosis method using unsupervised feature learning. J. Big Data 6, 32. https://doi.org/10.1186/s40537-019-0190-7.
Sabuncu, Mert R., et al., 2011. The dynamics of cortical and hippocampal atrophy in Alzheimer disease. Arch. Neurol. vol. 68 (8), 1040–1048. https://doi.org/10.1001/archneurol.2011.167.
Salunkhe, Sumit, et al., 2021. Classification of Alzheimer's disease patients using texture analysis and machine learning. Appl. Syst. Innov. 4 (3), 49.
Salvatore, Christian, et al., 2015. Magnetic resonance imaging biomarkers for the early diagnosis of Alzheimer's disease: a machine learning approach (Sep). Front. Neurosci. vol. 9 (307), 1. https://doi.org/10.3389/fnins.2015.00307 (Sep).
Sarica, Alessia, et al., 2017. Random forest algorithm for the classification of neuroimaging data in Alzheimer's disease: a systematic review, 6 Oct Front. Aging Neurosci. vol. 9, 329. https://doi.org/10.3389/fnagi.2017.00329, 6 Oct.
Alam, Saruar, Kwon, Goo-Rak, 2017. Alzheimer 's Disease Neuroimaging Initiative. 2017. Alzheimer disease classification using KPCA, LDA, and multi-kernel learning SVM. Int. J. Imaging Syst. Technol. 27 (2), 133–143. https://doi.org/10.1002/ima.22217.
Schmidt, Mike F., et al., 2018. A comparison of manual tracing and FreeSurfer for estimating hippocampal volume over the adult lifespan. Hum. Brain Mapp. vol. 39 (6), 2500–2513. https://doi.org/10.1002/hbm.24017.
Seyedi, Somayyeh, et al., 2020. Comparing VBM and ROI analyses for detection of gray matter abnormalities in patients with bipolar disorder using MRI. Middle East Curr. Psychiatry 27 (1), 1–7.
Shanmuganathan, Subana, 2016. Artificial neural network modelling: an introduction. Artificial Neural Network Modelling. Springer,, Cham, pp. 1–14.
Shattuck, David W., et al., 2008. Construction of a 3D probabilistic atlas of human cortical structures. NeuroImage vol. 39 (3), 1064–1080. https://doi.org/10.1016/j.neuroimage.2007.09.031.
Simões, Rita, et al., 2014. Classification and localization of early-stage Alzheimer's disease in magnetic resonance images using a patch-based classifier ensemble. Neuroradiology vol. 56 (9), 709–721. https://doi.org/10.1007/s00234-014-1385-4.
Singh, Vivek, et al., 2006. Spatial patterns of cortical thinning in mild cognitive impairment and Alzheimer's disease. Brain: a J. Neurol. vol. 129 (Pt 11), 2885–2893. https://doi.org/10.1093/brain/awl256.
Sørensen, L., Igel, C., Pai, A., et al., 2016. Differential diagnosis of mild cognitive impairment and Alzheimer's disease using structural MRI cortical thickness, hippocampal shape, hippocampal texture, and volumetry. Published 2016 Dec 7 Neuroimage Clin. 13, 470–482. https://doi.org/10.1016/j.nicl.2016.11.025.
Sørensen, Lauge, et al., 2012. Texture-based analysis of COPD: a data-driven approach. IEEE Trans. Med. Imaging vol. 31 (1), 70–78. https://doi.org/10.1109/TMI.2011.2164931.
Sperling, Reisa A., et al., 2011. Toward defining the preclinical stages of Alzheimer's disease: recommendations from the National Institute on Aging-Alzheimer's Association workgroups on diagnostic guidelines for Alzheimer's disease. Alzheimer'S. Dement.: J. Alzheimer'S. Assoc. vol. 7 (3), 280–292. https://doi.org/10.1016/j.jalz.2011.03.003.
Sur, Cyrille, et al., 2020. BACE inhibition causes rapid, regional, and non-progressive volume reduction in Alzheimer's disease brain. B*rain: a J. Neurol.* vol. 143 (12), 3816–3826. https://doi.org/10.1093/brain/awaa332.
Szczypiński, Piotr M., et al., 2009. MaZda—a software package for image texture analysis. Comput. Methods Prog. Biomed. 94 (1), 66–76.
Tanabe, J.L., et al., 1997. Tissue segmentation of the brain in Alzheimer disease. AJNR Am. J. Neuroradiol. vol. 18 (1), 115–123.
Tang, Xiaoying, et al., 2014. Shape abnormalities of subcortical and ventricular structures in mild cognitive impairment and Alzheimer's disease: detecting, quantifying, and predicting. Hum. Brain Mapp. 35 (8), 3701–3725.
Teipel, Stefan J., et al., 2007. Multivariate deformation-based analysis of brain atrophy to predict Alzheimer's disease in mild cognitive impairment. NeuroImage vol. 38 (1), 13–24. https://doi.org/10.1016/j.neuroimage.2007.07.008.
Teipel, Stefan J., et al., 2013. Relevance of magnetic resonance imaging for early detection and diagnosis of Alzheimer disease. Med. Clin. North Am. vol. 97 (3), 399–424. https://doi.org/10.1016/j.mcna.2012.12.013.
Testa, Cristina, et al., 2004. A comparison between the accuracy of voxel-based morphometry and hippocampal volumetry in Alzheimer's disease. J. Magn. Reson. Imaging.: Off. J. Int. Soc. Magn. Reson. Med. 19 (3), 274–282.
Toews, Matthew, et al., 2010. Feature-based morphometry: discovering group-related anatomical patterns. NeuroImage vol. 49 (3), 2318–2327. https://doi.org/10.1016/j.neuroimage.2009.10.032.
Tooba Altaf, S.Anwar, Nadia Gul, N. Majeed, and M. Majid. Multi-class alzheimer disease classification using hybrid features. In Proceedings of the Future Technologies Conference (FTC), 2017.
Trevethan, R., 2017. Sensitivity, specificity, and predictive values: foundations, pliabilities, and pitfalls in research and practice. Nov 20 Front Public Health 5, 307. https://doi.org/10.3389/fpubh.2017.00307.
Tzourio-Mazoyer, N., et al., 2002. Automated anatomical labeling of activations in SPM using a macroscopic anatomical parcellation of the MNI MRI single-subject brain. NeuroImage vol. 15 (1), 273–289. https://doi.org/10.1006/nimg.2001.0978.
Uysal, Gokce, Ozturk, Mahmut, 2020. Hippocampal atrophy-based Alzheimer's disease diagnosis via machine learning methods. J. Neurosci. Methods vol. 337, 108669. https://doi.org/10.1016/j.jneumeth.2020.108669.
Vaithinathan, Krishnakumar, et al., 2019. A novel texture extraction technique with T1 weighted MRI for the classification of Alzheimer's disease. J. Neurosci. Methods vol. 318, 84–99. https://doi.org/10.1016/j.jneumeth.2019.01.011.
Valliani, A.A., Ranti, D., Oermann, E.K., 2019. Deep learning and neurology: a systematic review. Neurol. Ther. 8, 351–365. https://doi.org/10.1007/s40120-019-00153-8.
Valsasina, P., et al., 2012. Spatial normalization and regional assessment of cord atrophy: voxel-based analysis of cervical cord 3D T1-weighted images. " *Ajnr. Am. J. Neuroradiol.* vol. 33 (11), 2195–2200. https://doi.org/10.3174/ajnr.A3139.
Vemuri, Prashanthi, et al., 2008. Alzheimer's disease diagnosis in individual subjects using structural MR images: validation studies. NeuroImage vol. 39 (3), 1186–1197. https://doi.org/10.1016/j.neuroimage.2007.09.073.
Vemuri, Prashanthi, Clifford, R., Jack Jr, 2010. Role of structural MRI in Alzheimer's disease, 31 Aug Alzheimer'S. Res. Ther. vol. 2 (4), 23. https://doi.org/10.1186/alzrt47, 31 Aug.
Venneri, Annalena, 2007. Imaging treatment effects in Alzheimer's disease. Magn. Reson. Imaging vol. 25 (6), 953–968. https://doi.org/10.1016/j.mri.2007.02.004.
Venugopalan, Janani, et al., 2021. Multimodal deep learning models for early detection of Alzheimer's disease stage, 5 Feb Sci. Rep. vol. 11 (1), 3254. https://doi.org/10.1038/s41598-020-74399-w, 5 Feb.
Vogelstein, J.T., Bridgeford, E.W., Tang, M., et al., 2021. Supervised dimensionality reduction for big data. Nat. Commun. 12, 2872. https://doi.org/10.1038/s41467-021-23102-2.
Wachinger, Christian, et al., 2016. Whole-brain analysis reveals increased neuroanatomical asymmetries in dementia for hippocampus and amygdala. Brain: a J. Neurol. vol. 139 (Pt 12), 3253–3266. https://doi.org/10.1093/brain/aww243.
Wang, Lei, et al., 2006. Abnormalities of hippocampal surface structure in very mild dementia of the Alzheimer type. NeuroImage vol. 30 (1), 52–60. https://doi.org/10.1016/j.neuroimage.2005.09.017.
Wang, Lei, et al., 2007. Large deformation diffeomorphism and momentum based hippocampal shape discrimination in dementia of the Alzheimer type. IEEE Trans. Med. Imaging vol. 26 (4), 462–470. https://doi.org/10.1109/TMI.2005.853923.
Wang, N., Chen, J., Xiao, H., et al., 2019. Application of artificial neural network model in diagnosis of Alzheimer's disease. BMC Neurol. 19, 154. https://doi.org/10.1186/s12883-019-1377-4.
Wang, Yandan, et al. "Lbp with six intersection points: Reducing redundant information in lbp-top for micro-expression recognition." Asian conference on computer vision. Springer, Cham, 2014.
Wang, Yu-Xiong, Zhang, Yu-Jin, 2012. Nonnegative matrix factorization: a comprehensive review. IEEE Trans. Knowl. Data Eng. 25 (6), 1336–1353.
Wee, Chong-Yaw, et al., 2013. Prediction of Alzheimer's disease and mild cognitive impairment using cortical morphological patterns. Hum. brain Mapp. vol. 34 (12), 3411–3425. https://doi.org/10.1002/hbm.22156.
Weiner, Michael W., et al., 2015. 2014 update of the Alzheimer's disease neuroimaging initiative: a review of papers published since its inception. Alzheimer's Dement.: J. Alzheimer's Assoc. vol. 11 (6), e1–120. https://doi.org/10.1016/j.jalz.2014.11.001.
Wilson, Stewart W., 1995. Classifier fitness based on accuracy. Evolut. Comput. 3 (2), 149–175.
Xiao, Zhe, et al., 2017. Brain MR image classification for Alzheimer's disease diagnosis based on multifeature fusion. Comput. Math. Methods Med. vol. 2017, 1952373. https://doi.org/10.1155/2017/1952373.
Yang, Huanqing, et al., 16 . 2019. Study of brain morphology change in Alzheimer's disease and amnestic mild cognitive impairment compared with normal controls. Gen. Psychiatry vol. 32 (2), e100005. https://doi.org/10.1136/gpsych-2018-100005.
Ye, J., Chen, K., Wu, T., Li, J., Zhao, Z., Patel, R., Bae, M., Janardan, R., Liu, H., Alexander, G., Reiman, E., 2008. Heterogeneous data fusion for Alzheimer's disease study. KDD'08: Proceeding of the 14th ACM SIGKDD International Conference on Knowledge Discovery and Data Mining, August 2008 Pages 1025–1033⟨https://doi.org/10.1145/1401890.1402012⟩.
Yeo, B.T. Thomas, et al., 2008. Effects of registration regularization and atlas sharpness on segmentation accuracy. Med. Image Anal. vol. 12 (5), 603–615. https://doi.org/10.1016/j.media.2008.06.005.
Yesavage, J.A., Brooks 3rd, J.O., 1991. On the importance of longitudinal research in Alzheimer's disease. J. Am. Geriatr. Soc. vol. 39 (9), 942–944. https://doi.org/10.1111/j.1532-5415.1991.tb04464.x.
Yushkevich, Paul A., et al., 2016. ITK-SNAP: an interactive tool for semi-automatic segmentation of multi-modality biomedical images. Annu. Int. Conf. IEEE Eng. Med. Biol. Soc. IEEE Eng. Med. Biol. Soc. Annu. Int. Conf. vol. 2016, 3342–3345. https://doi.org/10.1109/EMBC.2016.7591443.
Zhang, Daoqiang, et al., 2011. Multimodal classification of Alzheimer's disease and mild cognitive impairment. NeuroImage vol. 55 (3), 856–867. https://doi.org/10.1016/j.neuroimage.2011.01.008.
Zhang, Dengsheng, 2019. Wavelet transform. Fundamentals of image data mining. Springer,, Cham, pp. 35–44.
Zhang, J., Yu, C., Jiang, G., et al., 2012. 3D texture analysis on MRI images of Alzheimer's disease. Brain Imaging Behav. 6, 61–69.

Zhang, J., Liu, M., Le An, Y., Gao, D., Shen, 2017. Alzheimer's disease diagnosis using landmark-based features from longitudinal structural MR images (Nov). " IEEE J. Biomed. Health Inform. vol. 21 (6), 1607–1616. https://doi.org/10.1109/JBHI.2017.2704614.

Zhang, S., 2001. Challenges in KNN classification. " IEEE Trans. Knowl. Data Eng. https://doi.org/10.1109/TKDE.2021.3049250.

Zhang, Wang, et al., 2015. Detection of Alzheimer's disease and mild cognitive impairment based on structural volumetric MR images using 3D-DWT and WTA-KSVM trained by PSOTVAC. Biomed. Signal Process. Control 21, 58–73. https://doi.org/10.1016/j.bspc.2015.05.014.

Zhang, Yudong, et al., 2015. Detection of subjects and brain regions related to Alzheimer's disease using 3D MRI scans based on eigenbrain and machine learning (Jun). Front. Comput. Neurosci. vol. 9 (66), 2. https://doi.org/10.3389/fncom.2015.00066 (Jun).

Zhang, Zhongheng, 2016. Introduction to machine learning: k-nearest neighbors. Ann. Transl. Med. vol. 4 (11), 218. https://doi.org/10.21037/atm.2016.03.37.

Zilles, K., et al., 1988. The human pattern of gyrification in the cerebral cortex. Anat. Embryol. vol. 179 (2), 173–179. https://doi.org/10.1007/BF00304699.